Sains Malaysiana 53(12)(2024): 3437-3462
http://doi.org/10.17576/jsm-2024-5312-24

The One-Sided Variable Sampling Interval Exponentially Weighted Moving Average $\bar{X}$ Charts Under the Gamma Distribution

(Carta Purata Bergerak Berpemberat Eksponen Selang Pensampelan Berubah-ubah Satu Hala $\bar{X}$ di Bawah Taburan Gamma)

KAI LE GOH[1], WEI LIN TEOH[1,2,*], JING WEI TEOH[1], ZHI LIN CHONG[3] & XINYING CHEW[4]

[1]*School of Mathematical and Computer Sciences, Heriot-Watt University Malaysia, 62200 Putrajaya, Malaysia*
[2]*International Chair in Data Science & Explainable Artificial Intelligence, International Research Institute for Artificial Intelligence and Data Science, Dong A University, Danang, Vietnam*
[3]*Department of Electronic Engineering, Faculty of Engineering and Green Technology, Universiti Tunku Abdul Rahman, 31900 Kampar, Perak, Malaysia*
[4]*School of Computer Science, Universiti Sains Malaysia, 11800 Gelugor, Pulau Pinang, Malaysia*

Received: 26 July 2024/Accepted: 25 October 2024

ABSTRACT

Recently, adaptive quality control charts have been frequently utilised in diverse production and manufacturing industries to ensure process stability and maintain a desirable level of product quality. Among these charts, the variable sampling interval (VSI) exponentially weighted moving average (EWMA) $\bar{X}$ chart is known for its sensitivity and efficiency in monitoring the process mean shifts. However, the existing literature on the design of the VSI EWMA $\bar{X}$ chart is predicated on the presumption that the underlying process adheres to a normal distribution. This normality assumption is often violated in manufacturing settings, where many practical processes tend to follow non-normal or skewed distributions. Therefore, this paper investigates the performance of one-sided VSI EWMA $\bar{X}$ charts designed under the normal distribution model, when the quality characteristics of interest follow a gamma distribution. Our findings indicate that the in-control average time to signal and the standard deviation of the time to signal for the one-sided VSI EWMA $\bar{X}$ charts are significantly deteriorated under the gamma distribution. To tackle this problem, this paper proposes new charting parameters specifically derived for the one-sided VSI EWMA $\bar{X}$ charts under the gamma distribution. Besides, comparative analyses show that the proposed one-sided VSI EWMA $\bar{X}$ charts exhibit the best detection speed compared to the one-sided Shewhart $\bar{X}$ and EWMA $\bar{X}$ charts, when the process follows a gamma distribution. An illustrative application of the one-sided VSI EWMA $\bar{X}$ chart for monitoring the weight of bias tires in scooter manufacturing is provided at the end of this paper.

Keywords: Average time to signal; exponentially weighted moving average control chart; gamma distribution; statistical process control; variable sampling interval scheme

ABSTRAK

Baru-baru ini, carta kawalan kualiti beradaptif sering digunakan dalam pelbagai industri pengeluaran dan pembuatan untuk memastikan kestabilan proses dan mengekalkan tahap kualiti produk yang diinginkan. Antara carta ini, carta kawalan purata bergerak berpemberat eksponen selang pensampelan berubah-ubah (VSI EWMA) $\bar{X}$ dikenali kerana kepekaan dan kecekapannya dalam memantau perubahan min proses. Walau bagaimanapun, kepustakaan sedia ada yang mengenai reka bentuk carta VSI EWMA $\bar{X}$ adalah berdasarkan andaian bahawa proses asas mematuhi taburan normal. Andaian kenormalan ini sering tidak dipenuhi dalam persekitaran perbuatan dengan kebanyakan proses praktikal cendurung mengikuti taburan yang tidak normal atau taburan yang condong. Oleh itu, kertas ini mengkaji prestasi carta VSI EWMA $\bar{X}$ satu hala yang direka di bawah model taburan normal, apabila ciri kualiti yang diminati mengikuti taburan gamma. Hasil kajian menunjukkan bahawa purata masa untuk isyarat dan sisihan piawai masa untuk isyarat dalam kawalan bagi carta VSI EWMA $\bar{X}$ satu hala merosot dengan ketara di bawah taburan gamma. Untuk menangani masalah ini, kertas ini mencadangkan parameter carta baharu yang khususnya diperoleh untuk carta VSI EWMA $\bar{X}$ satu hala di bawah taburan gamma. Selain itu, analisis perbandingan menunjukkan bahawa carta VSI EWMA $\bar{X}$ satu hala yang dicadangkan mempunyai kelajuan pengesanan terbaik berbanding dengan carta Shewhart $\bar{X}$ dan EWMA $\bar{X}$ satu hala, apabila proses mengikuti taburan gamma. Satu aplikasi ilustrasi bagi carta VSI EWMA $\bar{X}$ satu hala untuk memantau berat tayar bias dalam pembuatan skuter disediakan pada bahagian akhir kertas ini.

Kata kunci: Carta kawalan purata bergerak berpemberat eksponen; kawalan proses statistik; purata masa untuk isyarat; skim selang pensampelan berubah-ubah; taburan gamma

INTRODUCTION

Statistical process control (SPC), known as a remarkable statistical approach in quality control, is extensively employed to control and monitor the manufacturing process. Through the application of various statistical methods, SPC strives to uphold and improve process quality by identifying trends, anomalies, and potential areas for improvement. Effective use of this technique ensures that the process operates at its optimum level and consistently produces high quality products. Within a range of advanced statistical tools in SPC, the quality control chart stands out as the most user-friendly and powerful approach in practical scenarios, due to its simplicity in analysis, visualisation, and fault detection. Contemporarily, many researchers, such as Sanmugan and Muzalwana (2022), Teh et al. (2015) and Teoh et al. (2024) just to mention a few, contribute valuably to the quality control charting enhancements in real-life settings, advancing methods for improved process stability and efficiency.

Among various types of control charts available in the SPC field, adaptive type control charts have garnered significant attention for their effectiveness in detecting assignable causes within processes. One of the prominent adaptive control charts is the variable sampling interval (VSI) exponentially weighted moving average (EWMA) $\bar{X}$ control chart. The construction of the VSI EWMA $\bar{X}$ chart involves integrating the VSI scheme with the EWMA $\bar{X}$ chart, thereby enhancing its effectiveness and sensitivity in identifying process mean shifts. Owing to this feature, the VSI EWMA type control chart is favoured among practitioners for its superior performance compared to other existing quality control charts, like the Shewhart, synthetic, supplementary run rules, and fixed sampling interval (FSI) EWMA control charts (Wang et al. 2020; Yeong et al. 2017). Furthermore, in scenarios involving estimated process parameters, Khoo et al. (2019) implemented the VSI EWMA median control chart, which generally outperforms the conventional Shewhart, EWMA, and VSI run sum median control charts in identifying changes of the mean shifts. This VSI EWMA median control chart also demonstrated high efficiency in monitoring the post-manufacturing waiting period for product shipment in an industrial setting. Subsequently, Teoh et al. (2021) optimised the VSI EWMA $\bar{X}$ control chart based on the normal distribution assumption and estimated process parameters, providing a more precise and specialised approach for process monitoring in practical situations. For effective process monitoring of both the mean and dispersion simultaneously under the normal distribution, Parvin et al. (2023) established maximum and distance EWMA charts that incorporate the VSI feature and account for unknown process parameters. These proposed charts have heightened sensitivity in detecting process changes and broadened the scope of quality control charts applications. In the context of industrial applications, the VSI EWMA chart has found widespread use in monitoring and controlling production and manufacturing processes. Example of recent applications include monitoring the weight of bottles in the milk bottle production process (Tran et al. 2020), monitoring the length, thickness, and inner diameter of carbon tubes in carbon fibre tubing manufacturing (Haq & Akhtar 2022), and monitoring the sintering process in mechanical manufacturing (Hu et al. 2024). Hence, given its proven effectiveness and extensive real-life applications, the VSI EWMA $\bar{X}$ control chart is considered for detailed investigation in this paper.

In the current SPC literature, numerous studies on the VSI EWMA $\bar{X}$ control chart are relied on the normal distribution model. Nevertheless, this model assumption often does not hold in practice, as many real-life processes exhibit skewed behaviour, rather than the normal distribution (Teoh et al. 2016). Specifically, the gamma distribution is frequently encountered in industrial contexts, such as in the measurement of particulate matter for air pollution (Nawaz, Azam & Aslam 2021), the weight of bias tires in scooter manufacturing (Lee et al. 2022), the product weight in multiheaded weighing machines used in packaging manufacturing (Madrid-Alvarez, García-Díaz & Tercero-Gómez 2024), and the wafer fabrication process in semiconductor manufacturing (Deenen et al. 2024). In process control operations, utilising control charts designed based on the normal distribution assumption to monitor the skewed processes can lead to degraded performance in the detection of assignable causes (Teoh et al. 2016). These control charts may not adequately capture variability and skewness of the process, increasing the likelihood of false alarms or undetected issues (Noorossana, Fathizadan & Nayebpour 2016). Besides, in order to monitor the non-normal processes, SPC researchers have developed three approaches; (1) The transformation method that transforms the non-normal data to normal data (Chou, Polansky & Mason 1998; Hamasha et al. 2022). For instance, Kao and Ho (2006) employed the transformation coefficient method to develop the S^2 control chart for controlling sample variances when the underlying process distribution is gamma. However, such a method could obscure the true underlying behaviour of the non-normal process, as the statistics of the control chart are transformed into a complex form, (2) To develop nonparametric control charts that are adaptable and compatible to various distributions without the presumption of normality (Chakraborti & Graham 2019; Chakraborti, Van Der Laan & Bakir 2001). For example, the nonparametric multivariate control chart using density-sensitive novelty weights has been proposed by Liu, Liu and Jung (2020) for effectively monitoring non-normal processes in modern manufacturing industry. Although the nonparametric method is effective for monitoring non-normal processes, it usually lacks the statistical power and is weaker than the parametric control chart when the underlying process distribution can be modelled accurately and conforms to typical statistical assumptions, and (3) Developing new control charting

parameters tailored to specific non-normal distributions (Bai et al. 2024; Li et al. 2014), which is employed in this paper for the gamma distribution. Instead of transforming data or using nonparametric methods (i.e., the first and second approaches), the third approach designs control charts that directly incorporate distribution-specific parameters for process like the gamma distribution. This method preserves the true behaviour of the non-normal process and retains the statistical power of parametric methods. By proposing new charting parameters tailored with a specific non-normal distribution, practitioners can simplify the operation and construction of the control chart, enhancing its interpretability and reducing overall complexity.

Due to the beneficial of the third approach, in this paper, we first conduct a comprehensive analysis on the performance of the one-sided VSI EWMA $\bar{X}$ chart, specifically when the quality characteristic of interest follows a gamma distribution. Particularly, both upper one-sided and lower one-sided VSI EWMA $\bar{X}$ charts are taken into consideration. The average time to signal (ATS) and standard deviation of the time to signal (SDTS) criteria are employed to examine both the in-control and out-of-control scenarios. Additionally, we propose new charting parameters for the one-sided VSI EWMA $\bar{X}$ charts, which are specifically adapted to the gamma distribution. These new charting parameters are intended to guide practitioners to achieve the highest level of effectiveness in detecting various process mean shifts under the gamma distribution. The proposed charts guarantee an excellent in-control performance and demonstrate enhanced detection speed for monitoring mean changes in a gamma-distributed process. Comparative studies are also performed to assess the effectiveness of the proposed one-sided VSI EWMA $\bar{X}$ control charts against other competing control charts.

The organisation of the remaining sections of this paper is outlined below. First, we present the operation framework of the two one-sided VSI EWMA $\bar{X}$ charts under the normal distribution model, along with its run-length properties. Subsequently, we discuss the statistical characteristic of the gamma distribution and assess how the two one-sided VSI EWMA $\bar{X}$ charts perform under the gamma distribution. We then introduce new charting parameters specifically derived for the two one-sided VSI EWMA $\bar{X}$ charts tailored for the gamma distribution, which are tabulated and discussed in detail. Following this, we conduct comparative studies among the one-sided Shewhart $\bar{X}$, EWMA $\bar{X}$, and VSI EWMA $\bar{X}$ charts under the gamma distribution. An illustrative application of the one-sided VSI EWMA $\bar{X}$ chart is demonstrated in the subsequent section. Last, we wrap up with a summary of findings and suggest research directions for future work.

THE ONE-SIDED VSI EWMA $\bar{X}$ CHARTS UNDER THE NORMAL DISTRIBUTION

In our context, let us define $X_{i,j}$ as the j^{th} observation from the i^{th} sample taken from a process, for subgroup number i= 1, 2, , and j = 1, 2, , n. Here, n represents the sample size. The observations $X_{i,j}$ are assumed to follow a normal distribution with an in-control mean (μ_0) and an in-control variance (σ_0^2), i.e., $X_{i,j} \sim N(\mu_0, \sigma_0^2)$, and are considered to be both independent and identically distributed. Following this, the two one-sided VSI EWMA $\bar{X}$ charts are constructed under this normal distribution model. The two one-sided VSI EWMA $\bar{X}$ charts comprise an upper one-sided chart for identifying positive mean shifts and a lower one-sided chart for identifying negative mean shifts. For the upper one-sided VSI EWMA $\bar{X}$ chart, its plotting statistic Z_i^+ at the i^{th} sample can be expressed as

$$Z_i^+ = \max[\mu_0, \lambda^+ \bar{X}_i + (1-\lambda^+) Z_{i-1}^+], \text{ for } i = 1, 2, \ldots, \quad (1)$$

where $\bar{X}_i = \sum_{j=1}^{n} X_{i,j}/n$ refers to the mean of the i^{th} sample. At the outset, the plotting statistics is initialised to $Z_0^+ = \mu_0$. The corresponding upper warning limit (UWL) and upper control limit (UCL) are given by

$$\text{UWL} = \mu_0 + W^+ \sqrt{\frac{\lambda^+}{n(2-\lambda^+)}}\sigma_0, \quad (2)$$

and

$$\text{UCL} = \mu_0 + K^+ \sqrt{\frac{\lambda^+}{n(2-\lambda^+)}}\sigma_0, \quad (3)$$

respectively. In Equations (1) – (3), λ^+ represents the smoothing parameter which satisfy $0 < \lambda^+ \leq 1$ while W^+ and K^+ are the coefficients for upper warning and upper control limits, respectively. It is important to point out that $W^+ \in (0, K^+)$.

For the lower one-sided VSI EWMA $\bar{X}$ chart, the plotting statistic (Z_i^-) can be defined as

$$Z_i^- = \min[\mu_0, \lambda^- \bar{X}_i + (1-\lambda^-) Z_{i-1}^-], \text{ for } i = 1, 2, \ldots, \quad (4)$$

with $Z_0^- = \mu_0$. The corresponding lower warning limit (LWL) and lower control limit (LCL) are

$$\text{LWL} = \mu_0 - W^- \sqrt{\frac{\lambda^-}{n(2-\lambda^-)}}\sigma_0, \quad (5)$$

and

$$\text{LCL} = \mu_0 - K^- \sqrt{\frac{\lambda^-}{n(2-\lambda^-)}}\sigma_0, \quad (6)$$

respectively. Here, λ^- represents the smoothing constant which satisfy $0 < \lambda^- \leq 1$. In Equations (5) and (6), W^- and K^- denote the coefficients for lower warning and lower control limits, respectively. They satisfy the condition $0 < W^- < K^-$. It should be noted that both the upper and lower one-sided VSI EWMA $\bar{X}$ charts have the same centre limit (CL), which is CL = μ_0.

Figure 1 provides a graphical representation of the upper and lower one-sided VSI EWMA $\bar{X}$ charts. From Figure 1(a), the upper one-sided VSI EWMA $\bar{X}$ chart is constructed by splitting it into three main regions, which are the safe region [CL, UWL], the warning region (UWL, UCL] and the out-of-control region (UCL, ∞). Similarly, referring to Figure 1(b), the lower one-sided VSI EWMA chart is built by dividing the chart into three key regions, which are the safe region [LWL, CL], the warning region [LCL, LWL), and the out-of-control region $(-\infty, \text{LCL})$. In this paper, we only consider two sampling intervals , which are the short sampling interval (h_S) and the long sampling interval (h_L), for these two one-sided VSI EWMA $\bar{X}$ charts. It should be emphasized that $h_S < h_L$. The adoption of only two sampling intervals is justified by Reynolds et al. (1988), who claimed that this approach effectively balances the detection speed and complexity of a VSI scheme control chart.

The proposed upper and lower one-sided VSI EWMA $\bar{X}$ charts are plotted simultaneously, allowing for the identification of both positive (upward) and negative (downward) process mean shifts. Outlined below are the implementation steps:

Step 1 Calculate the UWL, and UCL, for the upper one-sided VSI EWMA $\bar{X}$ chart, using Equations (2) and (3), respectively. Similarly, compute the LWL, and LCL, for the lower one-sided VSI EWMA $\bar{X}$ chart, using Equations (5) and (6), respectively.

Step 2 Collect a random sample consisting of n observations and determine the sample mean, $\bar{X}_i$.

Step 3 Compute Z_i^+ and Z_i^- using Equations (1) and (4), respectively

Step 4 Plot Z_i^+ and Z_i^- on the upper and lower one-sided VSI EWMA $\bar{X}$ charts, respectively.

Step 5 If Z_i^+ and Z_i^- lie within the safe regions [CL, UWL] and [LWL, CL], the process is concluded as in an in-control status, and the subsequent sample is drawn after a long sampling interval (h_L).

Step 6 If Z_i^+ and Z_i^- situate in the warning regions (UWL, UCL] and [LCL, LWL), the process remains as in an in-control status, and a short sampling interval (h_S) is utilised to take the next sample.

Step 7 The process is concluded to be in an out-of-control status if $Z_i^+ >$ UCL or $Z_i^- <$ LCL. Appropriate corrective measures must be executed, and any assignable causes must be identified and eliminated.

Typically, the operational performance of the FSI scheme control chart is assessed using the average run length (ARL) and the standard deviation of the run length (SDRL) criteria. Nevertheless, these ARL and SDRL metrics are unsuitable for the VSI scheme control chart due to the variation of time between two consecutive samples. Hence, the ATS and SDTS serve as more reliable indicators for measuring the effectiveness of the VSI scheme control chart. The ATS measures the average or

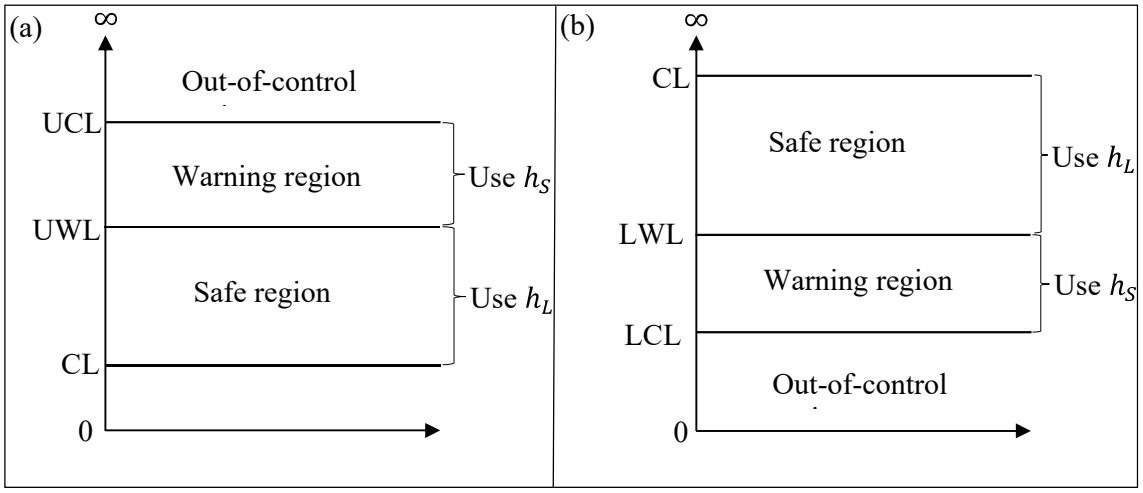

FIGURE 1. The graphical view of the operation for the (a) upper and (b) lower one-sided VSI EWMA $\bar{X}$ charts

anticipated time taken from the initial process monitoring until the VSI scheme control chart indicates the first out-of-control signal, whereas the SDTS denotes the variability or dispersion in the time to signal of the VSI scheme control chart.

To compute the ATS and SDTS of the one-sided VSI EWMA $\bar{X}$ chart, this paper adopts the Markov chain framework, initially introduced by Brook and Evans (1972). This approach is also widely employed by SPC researchers to assess and analyse the run-length characteristics of the VSI scheme control chart, as seen in the studies of Hu et al. (2023) and Xie et al. (2022). In this framework, the one-sided VSI EWMA $\bar{X}$ chart is represented as a discretized Markov chain model with (k + 2) states, assuming that states 0, 1, ..., k associate to the transient states. In the chain, the state k + 1 is defined as the absorbing state. As shown herewith, the complete transition probability matrix **P** is given as

$$\mathbf{P} = \begin{pmatrix} \mathbf{R} & \mathbf{r} \\ \mathbf{0}^T & 1 \end{pmatrix} = \begin{pmatrix} R_{0,0} & R_{0,1} & \cdots & R_{0,k} & r_0 \\ R_{1,0} & R_{1,1} & \cdots & R_{1,k} & r_1 \\ \vdots & \vdots & \ddots & \vdots & \vdots \\ R_{k,0} & R_{k,1} & \cdots & R_{k,k} & r_k \\ 0 & 0 & \cdots & 0 & 1 \end{pmatrix}. \quad (7)$$

Here, $\mathbf{0}$ = (0, 0, …, 0)T represents the column vector containing all zeros and **R** represents the (k + 1) × (k + 1) matrix that consists of transition probabilities $R_{u,v}$, for u,v = 0, 1, …, k. In Equation (7), **r = 1 - R1** denotes the column vector that ensures the sum of probabilities in each row equals 1, where **1** = (1, 1, …, 1)^T represents the (k + 1)-dimensional vector with all ones.

In order to calculate the probability matrix **R** in Equation (7), the transition probabilities $R_{u,v}$, for u,v = 0, 1, …, k, need to be identified. In the context of the upper one-sided VSI EWMA $\bar{X}$ chart, the interval between CL and UCL is partitioned into k subintervals, where each subinterval has a width 2d. Here, d = (UCL – CL)/2k. Similarly, the interval between CL and LCL of the lower one-sided VSI EWMA $\bar{X}$ chart is partitioned into k subintervals, each with a width of 2d, where d = (CL – LCL)/2k. Note that the number of subintervals is specified to be sufficiently large (k = 100) to ensure the accuracy of this finite method in evaluating the chart's performance. In our case, H_v, for v = 0, 1, …, k, is defined as the midpoint of the v^{th} subinterval $(H_v - d, H_v + d]$. When v = 0, this indicates that the charts return to a 'restart' state. Then, the generic element $R_{u,v}$, for u,v, = 0, 1, …, k, of the (k + 1) × (k + 1) transient probability matrix **R** can be expressed as follows.

- For the upper one-sided VSI EWMA $\bar{X}$ chart,

$$R_{u,v} = \begin{cases} \Phi\left(\left(\frac{\mu_0 - (1-\lambda^+)H_u}{\lambda^+} - \delta\right)\sqrt{n}\right) & , v = 0 \\ \Phi\left(\left(\frac{H_v + d - (1-\lambda^+)H_u}{\lambda^+} - \delta\right)\sqrt{n}\right) - \Phi\left(\left(\frac{H_v - d - (1-\lambda^+)H_u}{\lambda^+} - \delta\right)\sqrt{n}\right), & v \neq 0 \end{cases}. \quad (8)$$

- For the lower one-sided VSI EWMA $\bar{X}$ chart,

$$R_{u,v} = \begin{cases} 1 - \Phi\left(\left(\frac{\mu_0 - (1-\lambda^-)H_u}{\lambda^-} - \delta\right)\sqrt{n}\right) & , v = 0 \\ \Phi\left(\left(\frac{H_v + d - (1-\lambda^-)H_u}{\lambda^-} - \delta\right)\sqrt{n}\right) - \Phi\left(\left(\frac{H_v - d - (1-\lambda^-)H_u}{\lambda^-} - \delta\right)\sqrt{n}\right), & v \neq 0 \end{cases} \quad (9)$$

Here, $\Phi(\cdot)$ is defined as the standardised cumulative distribution function (cdf) of the normal distribution. In Equations (8) and (9), δ denotes the magnitude of the mean shift occurring in a process. If δ = 0, the process is considered as in-control, conversely, when $\delta \neq 0$, an out-of-control status is deemed.

Next, with the adoption of the Markov chain method, the ATS and SDTS of the one-sided VSI EWMA $\bar{X}$ chart can be calculated using the following expressions:

$$\text{ATS} = \mathbf{q}^T\mathbf{Q}\mathbf{b} - \mathbf{q}^T\mathbf{b} = \mathbf{q}^T(\mathbf{Q} - \mathbf{I})\mathbf{b}, \quad (10)$$

and

$$\text{SDTS} = \sqrt{\mathbf{q}^T\mathbf{Q}\mathbf{B}(2\mathbf{Q} - \mathbf{I})\mathbf{b} - (\mathbf{q}^T\mathbf{Q}\mathbf{b})^2}, \quad (11)$$

respectively, where the initial probability vector **q** = (1, 0, …, 0)^T represents the (k + 1) × 1 column vector with a unity in the first component and zeros elsewhere. In Equations (10) and (11), the matrix **Q** = (**I** - **R**)$^{-1}$ is the basic matrix, the matrix **I** indicates the (k + 1) × (k + 1) identity matrix, the vector **b** represents the (k + 1) × 1 vector comprising sampling intervals (with elements h_L or h_S) associated with the transient states in the discretized Markov chain model, and the matrix **B** is defined as a diagonal matrix, where the v^{th} component in matrix **B** is filled by b_v. Here, b_v = h_L if Z_i falls in the safe regions [CL, UWL] or [LWL, CL]; otherwise, b_v = h_S if Z_i is in the warning regions (UWL, UCL] or [LCL, LWL).

To make an unbiased analysis between the FSI and VSI scheme control charts, it is crucial to ensure that the in-control average sampling interval (ASI_0) values for both the one-sided VSI EWMA $\bar{X}$ charts and FSI scheme control charts are identical. The average sampling interval (ASI) can be determined using the following formula:

$$\text{ASI} = \frac{\mathbf{q}^T(\mathbf{I}-\mathbf{R})^{-1}\mathbf{b}}{\mathbf{q}^T(\mathbf{I}-\mathbf{R})^{-1}\mathbf{1}} \quad (12)$$

Note that same definitions of **q**, **I**, **R**, **b**, and **1** are followed here.

PERFORMANCE ANALYSIS OF THE ONE-SIDED VSI EWMA CHARTS $\bar{X}$ UNDER THE GAMMA DISTRIBUTION

This section starts with a discussion of the statistical properties of the gamma distribution. It is then followed by the comprehensive performance analysis of the one-sided VSI EWMA $\bar{X}$ charts under the gamma distribution.

For a gamma distribution, i.e., X~Gamma (a, b), the probability density function (pdf) is defined as $f(x) = x^{a-1}b^{-a}\exp(-x/b)/\Gamma(a)$, where a and $b$denotes the shape and scale parameters, respectively. It should be noticed that $x > 0, a > 0, b > 0$, and $\Gamma(\cdot)$ represents the gamma function. In the gamma distribution, the mean is given by $\mu = ab$ and the standard deviation is $\sigma = \sqrt{ab^2}$. Since the skewness of the gamma distribution is solely dependent on the shape parameter a, a decrease in the shape parameter a leads to an increase in the skewness of the gamma distribution. Throughout this paper, we specify $a \in \{1, 2, 4\}$ and $b = 1$ for simplicity.

Next, we investigate the in-control performance of both the upper and lower one-sided VSI EWMA $\bar{X}$ charts under the gamma distribution when the charting parameters are derived from the model based on the normal distribution assumption. Hence, some necessary prior specifications need to be set beforehand to obtain the charting parameters for the charts. We specify the in-control ATS (ATS_0) = 370.4, $ASI_0 = 1$, $n = 5$, and $\lambda = \{0.1, 0.2, 0.5\}$. In addition, we consider combinations of three sampling intervals $(h_S, h_L) \in \{(0.1, 1.5), (0.1, 1.9), (0.1, 4.0)\}$ for both the upper and lower one-sided VSI EWMA $\bar{X}$ charts (Teoh et al. 2021). The charting parameters (W^+, K^+) or (W^-, K^-) for the upper or lower one-sided VSI EWMA $\bar{X}$ charts are obtained under the normal distribution model using some non-linear equation solvers to meet the desired specifications. For illustration, when ATS_0 = 370.4, ASI_0 = 1, and n = 5, the charting parameters of the upper one-sided VSI EWMA $\bar{X}$ chart with (h_S, h_L) = (0.1, 1.9) and λ = 0.1 are obtained as (W^+, K^+) = (0.5911, 2.5800) under the normal distribution model. The charting parameters for both the upper and lower one-sided VSI EWMA $\bar{X}$ charts are tabulated in Table 1. In the following discussion, the in-control and out-of-control (ATS, STDS) values are referred to as (ATS_0, $SDTS_0$) and (ATS_1, $SDTS_1$) values, respectively.

Table 1 displays the (ATS_0, $SDTS_0$) values of the upper and lower one-sided VSI EWMA $\bar{X}$ charts under normal and specified gamma distributions using the same charting parameters. Since the formulae in Equations (10), (11), and (12) are not constructed based on the gamma distribution, all the computed (ATS, SDTS, ASI) values under the gamma distribution are obtained using Monte Carlo simulation involving 100,000 iterations throughout this paper. Based on Table 1, it is found that the (ATS_0, $SDTS_0$) values decrease for all the upper one-sided VSI EWMA $\bar{X}$ charts as the degree of skewness for the gamma distribution increases, deviating significantly from the nominal value of 370.4. As a numeric example, when λ = 0.2 and (h_S, h_L) = (0.1, 1.5), the (ATS_0, $SDTS_0$) values of the upper one-sided VSI EWMA $\bar{X}$ chart are (227.74, 227.53), (196.12, 195.98), and (164.97, 164.92) under Gamma (4, 1), Gamma (2, 1), and Gamma (1, 1) distributions, respectively, which show a considerable departure from the nominal value of 370.4. A substantial deterioration in the (ATS_0, $SDTS_0$) values is observed when λ increases, especially for λ = 0.5, indicating higher false alarms are signalled by the charts. This is unfavourable as the charts are ineffective and inefficient due to high false alarm rates. Besides, for the lower one-sided VSI EWMA $\bar{X}$ charts, Table 1 indicates that, an increase in the skewness of the gamma distribution results in a longer time to produce signals. This can be observed through the increase in the (ATS_0, $SDTS_0$) values (Table 1). When λ increases, the signalling time of the charts are relatively high as the skewness increases for the gamma distribution. For example, when λ = 0.5, the lower one-sided VSI EWMA $\bar{X}$ chart with (h_S, h_L) = (0.1, 1.9) shows (ATS_0, $SDTS_0$) = (6413.84, 6414.16) under the Gamma (2, 1) distribution. This significant difference might be due to the large variability between the normal and gamma distributions. Consequently, the (ATS_0, $SDTS_0$) values of the lower one-sided VSI EWMA $\bar{X}$ chart deviate substantially from the nominal value of 370.4, leading a delayed response to the actual behaviour of the process. Therefore, to address these problems, we propose new charting parameters for the one-sided VSI EWMA $\bar{X}$ charts specifically derived under the gamma distribution.

Table 2 and Figures 2 – 4 show the newly derived charting parameters of the one-sided VSI EWMA $\bar{X}$ charts against different a values of the gamma distribution for $\lambda \in \{0.1, 0.2, 0.5\}$, respectively. A description on the derivation for the new charting parameters of the one-sided VSI EWMA charts, is explained here. First, we adjust Equations (2), (3), (5), and (6) for the one-sided VSI EWMA $\bar{X}$ charts by substituting (μ_0, σ_0) with (μ, σ) of the gamma distribution. With these adjusted equations, the charting parameters (W^+, K^+) or (W^-, K^-) of the upper or lower one-sided VSI EWMA $\bar{X}$ charts are then determined using non-linear equation solvers to fulfil the required specifications, i.e., ATS_0 = 370.4, ASI_0 = 1, n = 5, and = {0.1, 0.2, 0.5} for different a values. Note that Monte Carlo simulation method is employed to determine the (ATS, SDTS) values under the gamma distribution. For ease of reproduction, visualisation and trend identification, these obtained charting parameters are provided in Table 2 and plotted according to the desired categories as shown in Figures 2 – 4. As a numeric illustration, under the predefined specifications with λ = 0.1, the charting parameters for the upper one-sided VSI EWMA $\bar{X}$ chart with (h_S, h_L) = (0.1, 1.5) are (W^+, K^+) ∈{(0.6159, 2.7864), (0.6299, 2.7948), (0.6241, 2.8185), (0.6167, 2.8552), (0.6039, 2.9361)} for {Gamma (5, 1), Gamma (4, 1), Gamma (3, 1), Gamma (2, 1), Gamma (1, 1)}, respectively (Table 2).

From Table 2, as well as Figures 2(a), 2(c), 3(a), 3(c), 4(a), and 4(c), there are no obvious trends or patterns for the warning coefficients (W^+ or W^-) of each combination of sampling intervals, except for a sudden drop of the W^- value at a = 3 for the lower one-sided VSI EWMA $\bar{X}$ chart with (h_S, h_L) = (0.1, 4.0) and λ = 0.5. For most combinations of sampling intervals and λ values, the W^+ values lie between 0.58 and 0.66, while the W^- values range from

TABLE 1. The (ATS_0, $SDTS_0$) values of the upper and lower one-sided VSI EWMA $\bar{X}$ charts under normal and various gamma distributions with the charting parameters obtained using the normal distribution model, for $ATS_0 = 370.4$, $ASI_0 = 1$, and $n = 5$ when $(h_S, h_L) \in \{(0.1, 1.5), (0.1, 1.9), (0.1, 4.0)\}$ and $\lambda \in \{0.1, 0.2, 0.5\}$

	Upper One-sided Charts			Lower One-sided Charts		
(h_S, h_L)	(0.1, 1.5)	(0.1, 1.9)	(0.1, 4.0)	(0.1, 1.5)	(0.1, 1.9)	(0.1, 4.0)
	(W^+, K^+)	(W^+, K^+)	(W^+, K^+)	(W^-, K^-)	(W^-, K^-)	(W^-, K^-)
Distributions	(ATS_0, $SDTS_0$)	(ATS_0, $SDTS_0$)	(ATS_0, $SDTS_0$)	(ATS_0, $SDTS_0$)	(ATS_0, $SDTS_0$)	(ATS_0, $SDTS_0$)
			$\lambda = 0.1$			
	(0.6250, 2.6613)	(0.5911, 2.5800)	(0.6531, 2.2266)	(0.6250, 2.6613)	(0.5911, 2.5800)	(0.6531, 2.2266)
Normal (0, 1)	(370.40, 368.67)	(370.40, 368.88)	(370.40, 367.77)	(370.40, 368.87)	(370.40, 368.88)	(370.40, 367.77)
Gamma (4, 1)	(277.32, 276.10)	(286.68, 285.50)	(318.50, 316.51)	(551.54, 549.62)	(526.81, 524.89)	(455.31, 451.93)
Gamma (2, 1)	(251.96, 250.87)	(263.39, 262.34)	(303.11, 301.35)	(679.01, 676.91)	(632.97, 630.84)	(506.30, 502.56)
Gamma (1, 1)	(224.33, 223.39)	(237.76, 236.88)	(285.72, 284.27)	(964.41, 962.02)	(862.10, 859.67)	(603.64, 599.34)
			$\lambda = 0.2$			
	(0.6235, 2.7843)	(0.6201, 2.7012)	(0.6379, 2.4033)	(0.6235, 2.7843)	(0.6201, 2.7012)	(0.6379, 2.4033)
Normal (0, 1)	(370.40, 369.99)	(370.40, 370.04)	(370.40, 370.17)	(370.40, 369.99)	(370.40, 370.04)	(370.40, 370.17)
Gamma (4, 1)	(227.74, 227.53)	(239.21, 239.07)	(277.38, 277.50)	(792.50, 791.85)	(730.66, 730.03)	(574.86, 574.20)
Gamma (2, 1)	(196.12, 195.98)	(209.09, 209.03)	(253.70, 253.95)	(1235.11, 1234.34)	(1082.74, 1081.99)	(736.55, 735.68)
Gamma (1, 1)	(164.97, 164.92)	(178.96, 179.00)	(229.01, 229.43)	(2838.91, 2837.95)	(2249.87, 2248.90)	(1152.25, 1151.05)
			$\lambda = 0.5$			
	(0.5994, 2.8434)	(0.6251, 2.7619)	(0.5808, 2.5103)	(0.5995, 2.8434)	(0.6251, 2.7619)	(0.5808, 2.5103)
Normal (0, 1)	(370.40, 370.79)	(370.40, 370.92)	(370.40, 371.75)	(370.40, 370.79)	(370.40, 370.92)	(370.40, 371.75)
Gamma (4, 1)	(160.16, 160.64)	(172.52, 173.14)	(213.26, 214.76)	(2207.64, 2207.91)	(1841.41, 1841.81)	(1136.23, 1137.42)
Gamma (2, 1)	(128.78, 129.28)	(141.31, 141.96)	(184.48, 186.03)	(9166.10, 9166.30)	(6413.84, 6414.16)	(2562.70, 2563.82)
Gamma (1, 1)	(102.10, 102.64)	(114.24, 114.94)	(158.21, 159.81)	(547381.68, 547381.74)	(200797.82, 200798.00)	(19498.07, 19499.02)

0.40 to 0.70. Moreover, as shown in Figures 2(b), 3(b), and 4(b), the K^+ values vary between 2.20 and 3.70 across all combinations of sampling intervals. The K^+ value exhibits a decreasing trend as a increases, which is likely due to the decrease in the skewness of the gamma distribution. Meanwhile, referring to Figures 2(d), 3(d), and 4(d), for the K^- values, there are some increasing trends as the a value increases. The K^+ value exhibits a decreasing trend as a increases, which is likely due to the decrease in the skewness of the gamma distribution. Meanwhile, referring to Figures 2(d), 3(d), and 4(d), for the K^- values, there are some increasing trends as the a value increases. For any λ value, the K^- value generally lies between 1.90 and 2.70 for the lower one-sided VSI EWMA $\bar{X}$ charts for the selected sampling intervals. Note that these newly derived charting parameters, which are included in Table 2 and Figures 2 - 4, are intended to serve as references and selection guides for practitioners.

We further assess the out-of-control performances of the one-sided VSI EWMA $\bar{X}$ charts by using the charting parameters specifically derived under the gamma distribution. The (ATS_1, $SDTS_1$) values under Gamma (4, 1), Gamma (2, 1), and Gamma (1, 1) distributions, for the upper and lower one-sided VSI EWMA $\bar{X}$ charts, are tabulated in the right panel of Tables 3 – 5. The (ATS_1, $SDTS_1$) values are given for $\delta \in$ {–2.00, –1.50, –1.00, –0.75, –0.50, –0.25, –0.10, 0.10, 0.25, 0.50, 0.75, 1.00, 1.50, 2.00} and $(h_S, h_L) \in$ {(0.1, 1.5), (0.1, 1.9), (0.1, 4.0)}. Table 3 corresponds to $\lambda = 0.1$, Table 4 to $\lambda = 0.2$, and Table 5 to $\lambda = 0.5$. In view of the upper one-sided VSI EWMA $\bar{X}$ chart, for the cases of $\lambda = 0.1$ and 0.2, the chart with $(h_S, h_L) = (0.1, 1.5)$ predominantly outperforms other corresponding charts with $(h_S, h_L) = (0.1, 1.9)$ and (0.1, 4.0) for $\delta \leq 1.00$ across all the gamma distributions (Tables 3 & 4). For example, given $\lambda = 0.1$ and under the (1, 1) distribution, the (ATS_1, $SDTS_1$) = (69.59, 68.06) of the upper one-sided VSI EWMA $\bar{X}$ chart with $(h_S, h_L) = (0.1, 1.5)$ are the smallest compared to (ATS_1, $SDTS_1$) = (74.79, 73.23) and (98.57, 96.70) of the charts with $(h_S, h_L) = (0.1, 1.9)$ and (0.1, 4.0), respectively. When $\delta \geq 1.50$ (the large shift sizes), for $\lambda = 0.1$ and 0.2, all the upper one-sided VSI EWMA $\bar{X}$ charts are generally having identical detection performance for all the gamma distributions (Tables 3 & 4). When $\lambda = 0.5$ and $\delta \leq 0.50$, the upper one-sided VSI EWMA $\bar{X}$ chart with $(h_S, h_L) = (0.1, 1.5)$ exhibits the fastest detection speed among all the combinations of sampling intervals, for all the gamma distributions (Table 5). For $\delta = 0.75$, the upper one-sided VSI EWMA $\bar{X}$ charts with $(h_S, h_L) = (0.1, 1.5)$ and (0.1, 1.9) have comparable performance in terms of the (ATS_1, $SDTS_1$) values. As an example, when $\lambda = 0.5$, $\delta = 0.75$, and under Gamma (2, 1) distribution, the (ATS_1, $SDTS_1$) = (0.93, 0.94) and (0.94, 1.07) are obtained for the upper one-sided VSI EWMA $\bar{X}$ charts with $(h_S, h_L) = (0.1, 1.5)$ and (0.1, 1.9), respectively, which are quite similar. Overall, when $\lambda = 0.5$ and for large magnitude of positive shifts ($\delta \geq 1.00$), all the upper one-sided VSI EWMA $\bar{X}$ charts have similar detection performance under the gamma distribution (Table 5).

When considering the lower one-sided VSI EWMA $\bar{X}$ chart, for $\lambda = 0.1$ and $\delta \geq -1.00$, the chart with $(h_S, h_L) = (0.1, 1.5)$ exhibits the best detection performance compared to the other (h_S, h_L) combinations, across all the gamma distributions (Table 3). As a numeric example, under the Gamma (1, 1) distribution with $\lambda = 0.1$, the lower one-sided VSI EWMA $\bar{X}$ chart with $(h_S, h_L) = (0.1, 1.5)$ has (ATS_1, $SDTS_1$) = (7.11, 6.02) for $\delta = -0.25$, which are the smallest compared to the (ATS_1, $SDTS_1$) = (8.75, 7.54) and (16.16, 14.56) of the lower one-sided VSI EWMA $\bar{X}$ charts with $(h_S, h_L) = (0.1, 1.9)$ and (0.1, 4.0), respectively (Table 3). When $\delta = -1.50$, it is observed that the lower-sided VSI EWMA $\bar{X}$ charts with $(h_S, h_L) = (0.1, 1.5)$ and (0.1, 1.9) have similar (ATS_1, $SDTS_1$) performance, outperforming the chart with $(h_S, h_L) = (0.1, 4.0)$, for all the gamma distributions (Table 3). For large negative shifts ($\delta = -2.00$), all the combinations of the lower one-sided VSI EWMA $\bar{X}$ chart show comparable detection speed across all the gamma distributions. It is important to note that similar trends as $\lambda = 0.1$, are clearly observed when $\lambda = 0.2$ and 0.5.

COMPARATIVE STUDIES

This section examines and contrasts the performance of the one-sided VSI EWMA $\bar{X}$ charts in comparison with the one-sided Shewhart $\bar{X}$ and EWMA $\bar{X}$ charts under the gamma distribution. More information can be obtained from Borror, Montgomery and Runger (1999) and Lee and Zhang (2020), for further descriptions on the Shewhart $\bar{X}$ and EWMA $\bar{X}$ charts under the gamma distribution. Note that some modifications were made to these charts to allow a fair assessment with the proposed charts. Since the Shewhart $\bar{X}$ and EWMA $\bar{X}$ charts are not VSI scheme control charts, necessary adjustments in the computation of the (ATS, SDTS) values are required. The ATS and SDTS can be obtained by multiplying the ARL and SDRL with h, where h is the FSI (Sabahno & Eriksson 2024). To ensure an unbiased evaluation with the VSI EWMA $\bar{X}$ chart, we set $h = 1$, which is equivalent to $(h_S, h_L) = (1.0, 1.0)$. In addition, the computed (ATS_1, $SDTS_1$) values of the upper and lower one-sided Shewhart $\bar{X}$ charts in Table 3 are similar to those values in Tables 4 and 5.

Tables 3 - 5 compare the (ATS_1, $SDTS_1$) values of the upper and lower one-sided Shewhart $\bar{X}$ (the left panel), EWMA $\bar{X}$ (the middle panel), and VSI EWMA $\bar{X}$ charts (the right panel), given that $ATS_0 = 370.4$, $ASI_0 = 1$, $n = 5$, $\lambda \in$ {0.1, 0.2, 0.5}, and $\delta \in$ {–2.00, –1.50, –1.00, –0.75, –0.50, –0.25, –0.10, 0.10, 0.25, 0.50, 0.75, 1.00, 1.50, 2.00}, under the Gamma (4, 1), Gamma (2, 1), and Gamma (1, 1) distributions. Note that the charting parameters (W^+, K^+) and (W^-, K^-) of the upper and lower one-sided VSI EWMA $\bar{X}$ charts, respectively, under the gamma distributions, are obtained from Figures 2 - 4. For all levels of positive mean shifts, all the upper one-sided VSI EWMA $\bar{X}$ charts exhibit

TABLE 2. The newly derived charting parameters for the upper and lower one-sided VSI EWMA $\bar{X}$ charts obtained under various gamma distributions, for $ATS_0 = 370.4$, $ASI_0 = 1$, and $n = 5$, when $(h_S, h_L) \in \{(0.5, 1.5), (0.3, 1.7), (0.1, 1.3), (0.1, 1.5), (0.1, 1.9), (0.1, 4.0)\}$ and $\lambda \in \{0.1, 0.2, 0.5\}$

	Upper One-sided Chart					
(h_S, h_L)	(0.5, 1.5)	(0.3, 1.7)	(0.1, 1.3)	(0.1, 1.5)	(0.1, 1.9)	(0.1, 4.0)
Distributions	(W^+, K^+)	(W^+, K^+)	(W^+, K^+)	(W^+, K^+)	(W^+, K^+)	(W^+, K^+)
	$\lambda = 0.1$					
Gamma (5, 1)	(0.6291, 2.7094)	(0.6333, 2.6913)	(0.6157, 2.8471)	(0.6159, 2.7864)	(0.6202, 2.6813)	(0.6567, 2.3018)
Gamma (4, 1)	(0.6540, 2.7168)	(0.6318, 2.7036)	(0.6504, 2.8474)	(0.6299, 2.7948)	(0.6415, 2.6838)	(0.6638, 2.3093)
Gamma (3, 1)	(0.6421, 2.7384)	(0.6508, 2.7178)	(0.6213, 2.8812)	(0.6241, 2.8185)	(0.6486, 2.7009)	(0.6527, 2.3247)
Gamma (2, 1)	(0.6348, 2.7727)	(0.6346, 2.7552)	(0.6263, 2.9149)	(0.6167, 2.8552)	(0.6258, 2.7387)	(0.5769, 2.3815)
Gamma (1, 1)	(0.6230, 2.8487)	(0.6229, 2.8297)	(0.6158, 3.0001)	(0.6039, 2.9361)	(0.6060, 2.8169)	(0.6252, 2.4006)
	$\lambda = 0.2$					
Gamma (5, 1)	(0.6228, 2.9176)	(0.6284, 2.9000)	(0.6372, 3.0359)	(0.6251, 2.9808)	(0.6110, 2.8874)	(0.6207, 2.5421)
Gamma (4, 1)	(0.6015, 2.9445)	(0.5796, 2.9313)	(0.6121, 3.0669)	(0.6192, 3.0068)	(0.5943, 2.9118)	(0.6193, 2.5605)
Gamma (3, 1)	(0.6065, 2.9762)	(0.6229, 2.9547)	(0.5709, 3.1136)	(0.6113, 3.0431)	(0.6144, 2.9369)	(0.6121, 2.5856)
Gamma (2, 1)	(0.6101, 3.0322)	(0.6031, 3.0130)	(0.5974, 3.1659)	(0.5751, 3.1105)	(0.6133, 2.9903)	(0.6288, 2.6157)
Gamma (1, 1)	(0.6272, 3.1510)	(0.5957, 3.1350)	(0.6524, 3.2832)	(0.6398, 3.2166)	(0.5959, 3.1140)	(0.6157, 2.6997)
	$\lambda = 0.5$					
Gamma (5, 1)	(0.6004, 3.1385)	(0.6156, 3.1089)	(0.6417, 3.2388)	(0.6151, 3.1848)	(0.6064, 3.0885)	(0.6217, 2.7496)
Gamma (4, 1)	(0.6472, 3.1709)	(0.6182, 3.1491)	(0.6456, 3.2828)	(0.6364, 3.2206)	(0.6011, 3.1282)	(0.6264, 2.7766)
Gamma (3, 1)	(0.6435, 3.2295)	(0.6390, 3.2009)	(0.6310, 3.3458)	(0.6412, 3.2810)	(0.6078, 3.1812)	(0.5851, 2.8298)
Gamma (2, 1)	(0.6352, 3.3284)	(0.6258, 3.2978)	(0.6525, 3.4454)	(0.6268, 3.3833)	(0.6089, 3.2730)	(0.6121, 2.8915)
Gamma (1, 1)	(0.6093, 3.5489)	(0.6282, 3.5064)	(0.6408, 3.6788)	(0.6439, 3.5989)	(0.6218, 3.4721)	(0.6119, 3.0413)

continue to next page

continue from previous page

	Lower One-sided Chart					
(h_S, h_L)	(0.5, 1.5)	(0.3, 1.7)	(0.1, 1.3)	(0.1, 1.5)	(0.1, 1.9)	(0.1, 4.0)
Distributions	(W^-, K^-)	(W^-, K^-)	(W^-, K^-)	(W^-, K^-)	(W^-, K^-)	(W^-, K^-)
	$\lambda = 0.1$					
Gamma (5, 1)	(0.6165, 2.4771)	(0.6458, 2.4590)	(0.6296, 2.5853)	(0.6265, 2.5405)	(0.6003, 2.4640)	(0.6180, 2.1640)
Gamma (4, 1)	(0.6245, 2.4616)	(0.6278, 2.4525)	(0.6301, 2.5713)	(0.6221, 2.5272)	(0.6353, 2.4400)	(0.6117, 2.1554)
Gamma (3, 1)	(0.6363, 2.4401)	(0.6349, 2.4309)	(0.6481, 2.5437)	(0.6522, 2.4967)	(0.6264, 2.4221)	(0.6208, 2.1386)
Gamma (2, 1)	(0.6220, 2.4079)	(0.6476, 2.3939)	(0.6267, 2.5130)	(0.6500, 2.4606)	(0.6361, 2.3884)	(0.6279, 2.1132)
Gamma (1, 1)	(0.6331, 2.3313)	(0.6836, 2.3106)	(0.6490, 2.4228)	(0.6380, 2.3872)	(0.6591, 2.3069)	(0.6657, 2.0420)
	$\lambda = 0.2$					
Gamma (5, 1)	(0.6324, 2.5392)	(0.6165, 2.5313)	(0.6078, 2.6372)	(0.6116, 2.5951)	(0.6143, 2.5219)	(0.6385, 2.2672)
Gamma (4, 1)	(0.6131, 2.5201)	(0.6036, 2.5134)	(0.6214, 2.6092)	(0.6283, 2.5679)	(0.5984, 2.5053)	(0.6258, 2.2555)
Gamma (3, 1)	(0.6303, 2.4860)	(0.6270, 2.4765)	(0.6202, 2.5770)	(0.6049, 2.5399)	(0.6148, 2.4703)	(0.6425, 2.2242)
Gamma (2, 1)	(0.6295, 2.4335)	(0.6388, 2.4227)	(0.6265, 2.5181)	(0.6321, 2.4801)	(0.6365, 2.4138)	(0.6340, 2.1876)
Gamma (1, 1)	(0.6277, 2.3182)	(0.6288, 2.3114)	(0.6343, 2.3926)	(0.6284, 2.3613)	(0.6420, 2.2999)	(0.6480, 2.0941)
	$\lambda = 0.5$					
Gamma (5, 1)	(0.5994, 2.4732)	(0.6263, 2.4574)	(0.6213, 2.5369)	(0.6253, 2.5028)	(0.6111, 2.4475)	(0.6550, 2.2429)
Gamma (4, 1)	(0.6362, 2.4324)	(0.6302, 2.4205)	(0.6161, 2.4990)	(0.6172, 2.4660)	(0.6455, 2.4057)	(0.6472, 2.2151)
Gamma (3, 1)	(0.6375, 2.3779)	(0.6264, 2.3679)	(0.6470, 2.4377)	(0.6476, 2.4065)	(0.6186, 2.3591)	(0.4351, 2.2120)
Gamma (2, 1)	(0.6356, 2.2912)	(0.6488, 2.2790)	(0.6386, 2.3467)	(0.6510, 2.3169)	(0.6434, 2.2691)	(0.6620, 2.0991)
Gamma (1, 1)	(0.6618, 2.1004)	(0.6591, 2.0924)	(0.6236, 2.1487)	(0.6500, 2.1240)	(0.6911, 2.0812)	(0.6388, 1.9518)

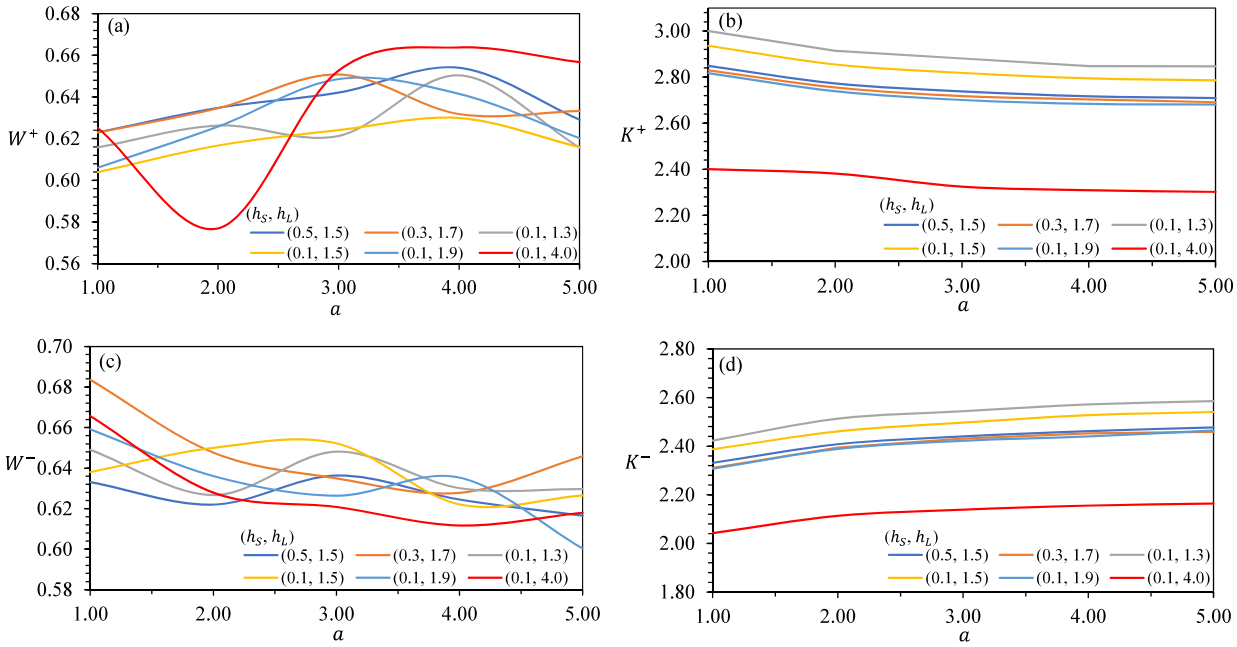

FIGURE 2. Plots of (a) W^+, and (b) K^+ values for the upper one-sided VSI EWMA $\bar{X}$ chart, as well as (c) W^-, and (d) K^- values for the lower one-sided VSI EWMA $\bar{X}$ chart against different a values of the gamma distribution, when $(h_S, h_L) \in \{(0.5, 1.5), (0.3, 1.7), (0.1, 1.3), (0.1, 1.5), (0.1, 1.9), (0.1, 4.0)\}$ and $\lambda = 0.1$

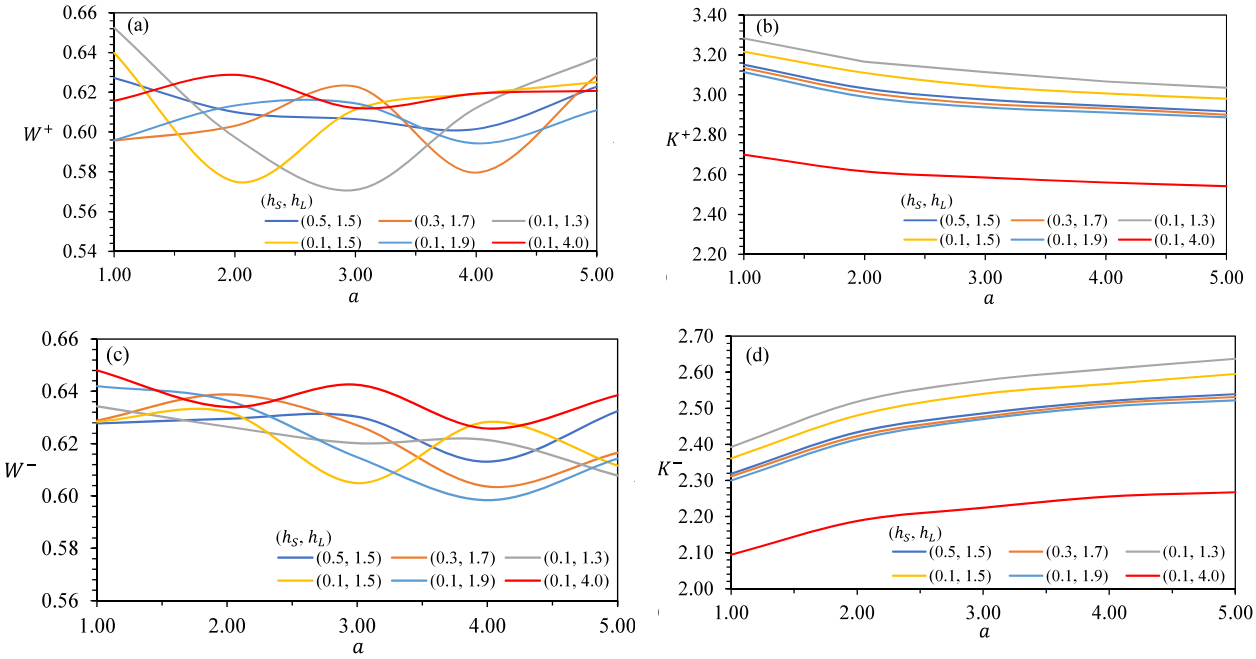

FIGURE 3. Plots of (a) W^+, and (b) K^+ values for the upper one-sided VSI EWMA $\bar{X}$ chart, as well as (c) W^-, and (d) K^- values for the lower one-sided VSI EWMA $\bar{X}$ chart against different a values of the gamma distribution, when $(h_S, h_L) \in \{(0.5, 1.5), (0.3, 1.7), (0.1, 1.3), (0.1, 1.5), (0.1, 1.9), (0.1, 4.0)\}$ and $\lambda = 0.2$

superior (ATS_1, $SDTS_1$) performances compared to the upper one-sided Shewhart $\bar{X}$ and EWMA $\bar{X}$ charts across all the gamma distributions, irrespective of the λ value (Tables 3 - 5). For instance, when $\delta = 0.5$ and $\lambda = 0.2$, the (ATS_1, $SDTS_1$) $\in$ {(2.37, 1.89), (2.53, 2.20), (4.40, 4.60)} are obtained for the upper one-sided VSI EWMA $\bar{X}$ charts with $(h_S, h_L) \in$ {(0.1, 1.5), (0.1, 1.9), (0.1, 4.0)}, under the Gamma (1, 1) distribution. These (ATS_1, $SDTS_1$) values are the lowest compared to the (ATS_1, $SDTS_1$) = (64.04, 63.53) and (10.67, 6.45) of the upper one-sided Shewhart $\bar{X}$ and EWMA $\bar{X}$ charts, respectively (Table 4). This signifies that the upper one-sided VSI EWMA $\bar{X}$ chart is the most powerful control chart compared to the upper one-sided Shewhart $\bar{X}$ and EWMA $\bar{X}$ charts in monitoring positive mean shifts of the gamma distribution. Moreover, it is crucial to notice that, for all levels of positive mean shifts, the detection efficiency of the upper one-sided EWMA $\bar{X}$ chart is greatly enhanced after incorporating the VSI feature across all the gamma distributions. As an example, when $\lambda = 0.2$ and $\delta = 0.10$, with the employment of $(h_S, h_L) = (0.1, 1.5)$, the (ATS_1, $SDTS_1$) of the upper one-sided EWMA $\bar{X}$ chart has reduced from (131.38, 126.85) to (96.51, 96.16), under the Gamma (2, 1) distribution (Table 4). This reveals that the upper one-sided VSI EWMA $\bar{X}$ chart has faster detection speed compared to the FSI scheme EWMA $\bar{X}$ chart under the gamma distribution.

Besides, we observe that, the upper one-sided VSI EWMA $\bar{X}$ chart with $(h_S, h_L) = (0.1, 1.5)$ and $\lambda = 0.1$ has the best detection performance compared to the upper one-sided Shewhart $\bar{X}$, EWMA $\bar{X}$ and other combinations of VSI EWMA $\bar{X}$ charts across all the gamma distributions for $\delta \leq 0.50$ (Table 3). This indicates that the upper one-sided VSI EWMA $\bar{X}$ chart with $(h_S, h_L) = (0.1, 1.5)$ and $\lambda = 0.1$, is the most effective chart for detecting small levels of positive mean shifts among all the comparing charts. For moderate positive mean shifts, i.e., $0.75 \leq \delta \leq 1.00$, the upper one-sided VSI EWMA $\bar{X}$ chart with $(h_S, h_L) = (0.1, 1.5)$ and $\lambda = 0.2$ offers the most effective performance compared to the upper one-sided Shewhart $\bar{X}$, EWMA $\bar{X}$, and other combinations of VSI EWMA $\bar{X}$ charts for all the gamma distributions (Table 4). From Table 5, all the combinations of (h_S, h_L) for the upper one-sided VSI EWMA $\bar{X}$ charts with $\lambda = 0.5$ outperform the upper one-sided Shewhart $\bar{X}$, EWMA $\bar{X}$ and other combinations of VSI EWMA $\bar{X}$ charts for large magnitude of positive mean shifts ($\delta \geq 1.50$) across all the gamma distributions.

Referring to the lower one-sided charts, for all the negative mean shifts, all the VSI EWMA $\bar{X}$ charts generally have superior detection speed when comparing with the Shewhart $\bar{X}$ and EWMA $\bar{X}$ charts across all the gamma distributions, regardless of the λ value (Tables 3 - 5). For example, under the Gamma (4, 1) distribution, when δ =

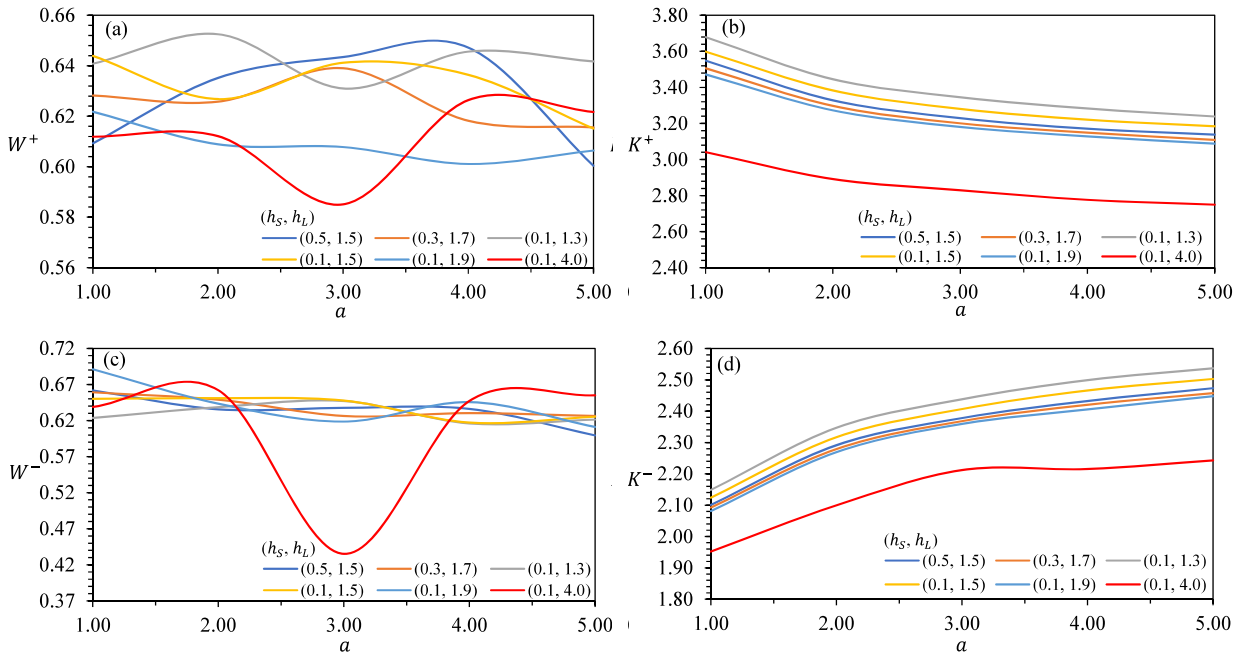

FIGURE 4. Plots of (a) W^+, and (b) K^+ values for the upper one-sided VSI EWMA $\bar{X}$ chart, as well as (c) , W^- and (d) K^- values for the lower one-sided VSI EWMA $\bar{X}$ chart against different a values of the gamma distribution, when $(h_S, h_L) \in$ {(0.5, 1.5), (0.3, 1.7), (0.1, 1.3), (0.1, 1.5), (0.1, 1.9), (0.1, 4.0)} and $\lambda = 0.5$

TABLE 3. The (ATS_1, $SDTS_1$) values of the upper and lower one-sided Shewhart $\bar{X}$, EWMA $\bar{X}$, and VSI EWMA $\bar{X}$ charts, for $ATS_0 = 370.4$, $ASI_0 = 1$, $n = 5$, and $\delta \in \{-2.00, -1.50, -1.00, -0.75, -0.50, -0.25, -0.10, 0.10, 0.25, 0.50, 0.75, 1.00, 1.50, 2.00\}$, when $(h_S, h_L) \in \{(0.1, 1.5), (0.1, 1.9), (0.1, 4.0)\}$ and $\lambda = 0.1$ under Gamma (4, 1), Gamma (2, 1), and Gamma (1, 1) distributions

	Shewhart $\bar{X}$	EWMA $\bar{X}$	VSI EWMA $\bar{X}$		
(h_S, h_L)	(1.0, 1.0)	(1.0, 1.0)	(0.1, 1.5)	(0.1, 1.9)	(0.1, 4.0)
δ	Gamma (4, 1)				
	Upper One-sided Charts				
	$K^+ = 3.2848$	$K^+ = 2.7624$	$(W^+, K^+) = (0.6299, 2.7948)$	$(W^+, K^+) = (0.6415, 2.6838)$	$(W^+, K^+) = (0.6638, 2.3093)$
	(ATS_1, $SDTS_1$)	(ATS_1, $SDTS_1$)	(ATS_1, $SDTS_1$)	(ATS_1, $SDTS_1$)	(ATS_1, $SDTS_1$)
0.10	(230.65, 230.15)	(93.34, 84.97)	(61.19, 59.55)	(67.01, 65.25)	(90.83, 88.53)
0.25	(116.44, 115.94)	(24.17, 16.68)	(9.04, 7.49)	(10.78, 9.20)	(19.51, 17.69)
0.50	(40.31, 39.81)	(8.69, 3.73)	(2.51, 1.93)	(3.02, 2.45)	(5.67, 5.17)
0.75	(15.57, 15.06)	(5.24, 1.69)	(1.19, 1.04)	(1.42, 1.33)	(2.60, 2.84)
1.00	(6.81, 6.29)	(3.80, 1.02)	(0.61, 0.66)	(0.71, 0.86)	(1.22, 1.84)
1.50	(2.01, 1.42)	(2.54, 0.57)	(0.18, 0.18)	(0.18, 0.24)	(0.19, 0.52)
2.00	(1.12, 0.37)	(2.00, 0.29)	(0.10, 0.03)	(0.10, 0.03)	(0.08, 0.05)
	Lower One-sided Charts				
	$K^- = 2.2861$	$K^- = 2.4854$	$(W^-, K^-) = (0.6221, 2.5272)$	$(W^-, K^-) = (0.6353, 2.4400)$	$(W^-, K^-) = (0.6117, 2.1554)$
	(ATS_1, $SDTS_1$)	(ATS_1, $SDTS_1$)	(ATS_1, $SDTS_1$)	(ATS_1, $SDTS_1$)	(ATS_1, $SDTS_1$)
–0.10	(132.29, 131.78)	(69.41, 60.69)	(44.17, 42.43)	(49.57, 47.68)	(69.90, 67.58)
–0.25	(38.30, 37.79)	(18.61, 11.95)	(7.63, 6.45)	(9.21, 7.98)	(16.19, 14.94)
–0.50	(8.87, 8.36)	(7.35, 3.09)	(2.25, 1.91)	(2.74, 2.43)	(4.92, 4.96)
–0.75	(3.49, 2.95)	(4.61, 1.51)	(1.06, 1.07)	(1.28, 1.37)	(2.21, 2.83)
–1.00	(1.96, 1.37)	(3.40, 0.96)	(0.56, 0.69)	(0.66, 0.90)	(1.06, 1.84)
–1.50	(1.17, 0.44)	(2.31, 0.51)	(0.19, 0.29)	(0.20, 0.38)	(0.26, 0.76)
–2.00	(1.02, 0.16)	(1.93, 0.35)	(0.10, 0.10)	(0.10, 0.13)	(0.08, 0.27)

continue to next page

continue from previous page

	Gamma (2, 1)				
	Upper One-sided Charts				
	$K^+ = 3.4912$	$K^+ = 2.8197$	$(W^+, K^+) = (0.6167, 2.8552)$	$(W^+, K^+) = (0.6258, 2.7387)$	$(W^+, K^+) = (0.5769, 2.3815)$
	$(ATS_1, SDTS_1)$	$(ATS_1, SDTS_1)$	$(ATS_1, SDTS_1)$	$(ATS_1, SDTS_1)$	$(ATS_1, SDTS_1)$
0.10	(243.26, 242.76)	(98.80, 90.53)	(64.47, 62.88)	(70.29, 68.61)	(89.31, 87.75)
0.25	(131.72, 131.22)	(25.53, 17.86)	(9.16, 7.54)	(10.88, 9.25)	(17.70, 16.37)
0.50	(49.86, 49.36)	(8.99, 3.87)	(2.51, 1.90)	(3.01, 2.41)	(4.97, 4.77)
0.75	(20.31, 19.80)	(5.38, 1.72)	(1.18, 1.01)	(1.40, 1.29)	(2.17, 2.56)
1.00	(9.02, 8.50)	(3.89, 1.03)	(0.60, 0.64)	(0.69, 0.82)	(0.94, 1.58)
1.50	(2.47, 1.90)	(2.59, 0.57)	(0.17, 0.13)	(0.17, 0.17)	(0.14, 0.24)
2.00	(1.19, 0.47)	(2.01, 0.29)	(0.10, 0.03)	(0.10, 0.03)	(0.08, 0.04)
	Lower One-sided Charts				
	$K^- = 2.0876$	$K^- = 2.4289$	$(W^-, K^-) = (0.6500, 2.4606)$	$(W^-, K^-) = (0.6361, 2.3884)$	$(W^-, K^-) = (0.6279, 2.1132)$
	$(ATS_1, SDTS_1)$	$(ATS_1, SDTS_1)$	$(ATS_1, SDTS_1)$	$(ATS_1, SDTS_1)$	$(ATS_1, SDTS_1)$
–0.10	(103.92, 103.42)	(65.08, 56.32)	(42.25, 40.37)	(46.46, 44.54)	(67.03, 64.52)
–0.25	(26.14, 25.63)	(17.65, 11.16)	(7.65, 6.45)	(8.89, 7.72)	(15.93, 14.64)
–0.50	(6.14, 5.62)	(7.09, 2.97)	(2.31, 1.95)	(2.68, 2.41)	(4.91, 4.97)
–0.75	(2.68, 2.12)	(4.48, 1.47)	(1.09, 1.10)	(1.25, 1.37)	(2.21, 2.86)
–1.00	(1.67, 1.06)	(3.32, 0.94)	(0.58, 0.73)	(0.65, 0.90)	(1.07, 1.88)
–1.50	(1.12, 0.37)	(2.28, 0.49)	(0.20, 0.32)	(0.20, 0.39)	(0.28, 0.81)
–2.00	(1.02, 0.14)	(1.90, 0.37)	(0.10, 0.13)	(0.10, 0.16)	(0.09, 0.32)

continue to next page

continue from previous page

	Gamma (1, 1)				
	Upper One-sided Charts				
	$K^+ = 3.7792$	$K^+ = 2.9000$	$(W^+, K^+) = (0.6039, 2.9361)$	$(W^+, K^+) = (0.6060, 2.8169)$	$(W^+, K^+) = (0.6252, 2.4006)$
	$(ATS_1, SDTS_1)$	$(ATS_1, SDTS_1)$	$(ATS_1, SDTS_1)$	$(ATS_1, SDTS_1)$	$(ATS_1, SDTS_1)$
0.10	(258.03, 257.53)	(106.72, 98.62)	(69.59, 68.06)	(74.79, 73.23)	(98.57, 96.70)
0.25	(151.42, 150.92)	(27.56, 19.66)	(9.40, 7.65)	(10.94, 9.22)	(19.59, 17.79)
0.50	(64.04, 63.53)	(9.44, 4.09)	(2.54, 1.86)	(2.98, 2.34)	(5.51, 4.95)
0.75	(28.21, 27.70)	(5.58, 1.77)	(1.18, 0.97)	(1.37, 1.23)	(2.47, 2.62)
1.00	(13.06, 12.55)	(4.00, 1.04)	(0.59, 0.60)	(0.66, 0.77)	(1.10, 1.68)
1.50	(3.43, 2.88)	(2.66, 0.57)	(0.17, 0.06)	(0.16, 0.07)	(0.13, 0.12)
2.00	(1.36, 0.70)	(2.03, 0.31)	(0.10, 0.03)	(0.10, 0.03)	(0.09, 0.04)
	Lower One-sided Charts				
	$K^- = 1.8200$	$K^- = 2.3500$	$(W^-, K^-) = (0.6380, 2.3872)$	$(W^-, K^-) = (0.6591, 2.3069)$	$(W^-, K^-) = (0.6657, 2.0420)$
	$(ATS_1, SDTS_1)$	$(ATS_1, SDTS_1)$	$(ATS_1, SDTS_1)$	$(ATS_1, SDTS_1)$	$(ATS_1, SDTS_1)$
–0.10	(64.57, 64.07)	(59.37, 50.57)	(37.78, 35.92)	(43.33, 41.22)	(64.75, 61.63)
–0.25	(14.21, 13.70)	(16.40, 10.13)	(7.11, 6.02)	(8.75, 7.54)	(16.16, 14.56)
–0.50	(3.82, 3.29)	(6.76, 2.81)	(2.17, 1.90)	(2.70, 2.44)	(5.13, 5.08)
–0.75	(1.99, 1.41)	(4.31, 1.41)	(1.03, 1.08)	(1.26, 1.40)	(2.33, 2.96)
–1.00	(1.42, 0.77)	(3.21, 0.93)	(0.55, 0.71)	(0.66, 0.93)	(1.15, 1.98)
–1.50	(1.08, 0.30)	(2.23, 0.46)	(0.19, 0.33)	(0.22, 0.43)	(0.32, 0.91)
–2.00	(1.02, 0.13)	(1.85, 0.42)	(0.10, 0.14)	(0.10, 0.19)	(0.09, 0.40)

TABLE 4. The (ATS_1, $SDTS_1$) values of the upper and lower one-sided Shewhart $\bar{X}$, EWMA $\bar{X}$, and VSI EWMA $\bar{X}$ charts, for $ATS_0 = 370.4$, $ASI_0 = 1$, $n = 5$, and $\delta \in \{-2.00, -1.50, -1.00, -0.75, -0.50, -0.25, -0.10, 0.10, 0.25, 0.50, 0.75, 1.00, 1.50, 2.00\}$, when $(h_S, h_L) \in \{(0.1, 1.5), (0.1, 1.9), (0.1, 4.0)\}$ and $\lambda = 0.2$ under Gamma (4, 1), Gamma (2, 1), and Gamma (1, 1) distributions

	Shewhart $\bar{X}$	EWMA $\bar{X}$	VSI EWMA $\bar{X}$		
(h_S, h_L)	(1.0, 1.0)	(1.0, 1.0)	(0.1, 1.5)	(0.1, 1.9)	(0.1, 4.0)
δ	Gamma (4, 1)				
	Upper One-sided Charts				
	$K^+ = 3.2848$	$K^+ = 2.9896$	$(W^+, K^+) = (0.6192, 3.0068)$	$(W^+, K^+) = (0.5943, 2.9118)$	$(W^+, K^+) = (0.6193, 2.5605)$
	(ATS_1, $SDTS_1$)	(ATS_1, $SDTS_1$)	(ATS_1, $SDTS_1$)	(ATS_1, $SDTS_1$)	(ATS_1, $SDTS_1$)
0.10	(230.65, 230.15)	(121.96, 117.82)	(90.38, 89.96)	(93.76, 93.43)	(112.05, 112.03)
0.25	(116.44, 115.94)	(31.88, 27.03)	(13.09, 12.45)	(14.34, 13.81)	(22.32, 22.24)
0.50	(40.31, 39.81)	(8.97, 5.15)	(2.14, 1.87)	(2.41, 2.26)	(4.26, 4.69)
0.75	(15.57, 15.06)	(4.82, 1.97)	(0.85, 0.88)	(0.93, 1.08)	(1.57, 2.30)
1.00	(6.81, 6.29)	(3.33, 1.08)	(0.38, 0.48)	(0.40, 0.59)	(0.60, 1.27)
1.50	(2.01, 1.42)	(2.15, 0.52)	(0.12, 0.09)	(0.11, 0.10)	(0.10, 0.19)
2.00	(1.12, 0.37)	(1.72, 0.46)	(0.07, 0.05)	(0.07, 0.05)	(0.04, 0.05)
	Lower One-sided Charts				
	$K^- = 2.2861$	$K^- = 2.5441$	$(W^-, K^-) = (0.6283, 2.5679)$	$(W^-, K^-) = (0.5984, 2.5053)$	$(W^-, K^-) = (0.6258, 2.2555)$
	(ATS_1, $SDTS_1$)	(ATS_1, $SDTS_1$)	(ATS_1, $SDTS_1$)	(ATS_1, $SDTS_1$)	(ATS_1, $SDTS_1$)
–0.10	(132.29, 131.78)	(79.40, 74.15)	(56.76, 56.18)	(60.35, 59.88)	(79.43, 79.15)
–0.25	(38.30, 37.79)	(19.28, 14.86)	(8.62, 8.22)	(9.70, 9.43)	(16.49, 16.64)
–0.50	(8.87, 8.36)	(6.47, 3.40)	(1.85, 1.86)	(2.11, 2.25)	(3.92, 4.67)
–0.75	(3.49, 2.95)	(3.82, 1.53)	(0.76, 0.94)	(0.85, 1.15)	(1.54, 2.44)
–1.00	(1.96, 1.37)	(2.77, 0.91)	(0.37, 0.57)	(0.41, 0.69)	(0.67, 1.49)
–1.50	(1.17, 0.44)	(1.90, 0.53)	(0.12, 0.21)	(0.12, 0.26)	(0.14, 0.55)
–2.00	(1.02, 0.16)	(1.38, 0.49)	(0.04, 0.08)	(0.04, 0.09)	(0.03, 0.18)

continue to next page

continue from previous page

	Gamma (2, 1)				
	Upper One-sided Charts				
	$K^+ = 3.4912$	$K^+ = 3.0841$	$(W^+, K^+) = (0.5751, 3.1105)$	$(W^+, K^+) = (0.6133, 2.9903)$	$(W^+, K^+) = (0.6288, 2.6157)$
	$(ATS_1, SDTS_1)$	$(ATS_1, SDTS_1)$	$(ATS_1, SDTS_1)$	$(ATS_1, SDTS_1)$	$(ATS_1, SDTS_1)$
0.10	(243.26, 242.76)	(131.38, 126.85)	(96.51, 96.16)	(101.95, 101.63)	(119.88, 119.85)
0.25	(131.72, 131.22)	(35.32, 30.43)	(13.70, 13.03)	(15.74, 15.14)	(24.02, 23.83)
0.50	(49.86, 49.36)	(9.63, 5.64)	(2.11, 1.79)	(2.51, 2.28)	(4.40, 4.72)
0.75	(20.31, 19.80)	(5.07, 2.09)	(0.82, 0.83)	(0.97, 1.08)	(1.62, 2.29)
1.00	(9.02, 8.50)	(3.45, 1.12)	(0.36, 0.43)	(0.41, 0.58)	(0.59, 1.24)
1.50	(2.47, 1.90)	(2.21, 0.53)	(0.12, 0.06)	(0.12, 0.06)	(0.09, 0.10)
2.00	(1.19, 0.47)	(1.77, 0.43)	(0.08, 0.04)	(0.07, 0.05)	(0.05, 0.05)
	Lower One-sided Charts				
	$K^- = 2.0876$	$K^- = 2.4563$	$(W^-, K^-) = (0.6321, 2.4801)$	$(W^-, K^-) = (0.6365, 2.4138)$	$(W^-, K^-) = (0.6340, 2.1876)$
	$(ATS_1, SDTS_1)$	$(ATS_1, SDTS_1)$	$(ATS_1, SDTS_1)$	$(ATS_1, SDTS_1)$	$(ATS_1, SDTS_1)$
–0.10	(103.92, 103.42)	(71.75, 66.42)	(50.88, 50.27)	(55.55, 54.97)	(73.90, 73.49)
–0.25	(26.14, 25.63)	(17.44, 13.12)	(7.91, 7.55)	(9.29, 9.00)	(15.66, 15.81)
–0.50	(6.14, 5.62)	(6.08, 3.14)	(1.79, 1.84)	(2.14, 2.30)	(3.89, 4.67)
–0.75	(2.68, 2.12)	(3.65, 1.46)	(0.75, 0.94)	(0.88, 1.20)	(1.55, 2.48)
–1.00	(1.67, 1.06)	(2.68, 0.87)	(0.37, 0.58)	(0.42, 0.74)	(0.70, 1.53)
–1.50	(1.12, 0.37)	(1.83, 0.55)	(0.12, 0.23)	(0.12, 0.30)	(0.15, 0.61)
–2.00	(1.02, 0.14)	(1.32, 0.48)	(0.04, 0.10)	(0.04, 0.12)	(0.03, 0.23)

continue to next page

continue from previous page

	Gamma (1, 1)				
	Upper One-sided Charts				
	$K^+ = 3.7792$	$K^+ = 3.2176$	$(W^+, K^+) = (0.6398, 3.2166)$	$(W^+, K^+) = (0.5959, 3.1140)$	$(W^+, K^+) = (0.6157, 2.6997)$
	$(ATS_1, SDTS_1)$	$(ATS_1, SDTS_1)$	$(ATS_1, SDTS_1)$	$(ATS_1, SDTS_1)$	$(ATS_1, SDTS_1)$
0.10	(258.03, 257.53)	(144.66, 140.34)	(110.13, 109.74)	(111.71, 111.46)	(129.52, 129.59)
0.25	(151.42, 150.92)	(40.67, 35.72)	(16.40, 15.59)	(17.06, 16.39)	(25.75, 25.48)
0.50	(64.04, 63.53)	(10.67, 6.45)	(2.37, 1.89)	(2.53, 2.20)	(4.40, 4.60)
0.75	(28.21, 27.70)	(5.43, 2.26)	(0.93, 0.86)	(0.96, 1.02)	(1.60, 2.18)
1.00	(13.06, 12.55)	(3.64, 1.17)	(0.40, 0.45)	(0.38, 0.50)	(0.53, 1.12)
1.50	(3.43, 2.88)	(2.29, 0.55)	(0.13, 0.06)	(0.12, 0.05)	(0.10, 0.05)
2.00	(1.36, 0.70)	(1.83, 0.38)	(0.08, 0.04)	(0.08, 0.04)	(0.06, 0.05)
	Lower One-sided Charts				
	$K^- = 1.8200$	$K^- = 2.3358$	$(W^-, K^-) = (0.6284, 2.3613)$	$(W^-, K^-) = (0.6420, 2.2999)$	$(W^-, K^-) = (0.6480, 2.0941)$
	$(ATS_1, SDTS_1)$	$(ATS_1, SDTS_1)$	$(ATS_1, SDTS_1)$	$(ATS_1, SDTS_1)$	$(ATS_1, SDTS_1)$
–0.10	(64.57, 64.07)	(61.86, 56.44)	(43.06, 42.44)	(47.90, 47.26)	(66.38, 65.79)
–0.25	(14.21, 13.70)	(15.19, 11.04)	(6.94, 6.65)	(8.31, 8.08)	(14.48, 14.62)
–0.50	(3.82, 3.29)	(5.57, 2.81)	(1.68. 1.78)	(2.04, 2.25)	(3.80, 4.61)
–0.75	(1.99, 1.41)	(3.42, 1.36)	(0.71, 0.94)	(0.85, 1.20)	(1.55, 2.51)
–1.00	(1.42, 0.77)	(2.56, 0.82)	(0.36, 0.58)	(0.42, 0.75)	(0.72, 1.58)
–1.50	(1.08, 0.30)	(1.73, 0.57)	(0.11, 0.25)	(0.12, 0.32)	(0.17, 0.68)
–2.00	(1.02, 0.13)	(1.25, 0.44)	(0.03, 0.11)	(0.03, 0.14)	(0.04, 0.29)

TABLE 5. The (ATS_1, $SDTS_1$) values of the upper and lower one-sided Shewhart $\bar{X}$, EWMA $\bar{X}$, and VSI EWMA $\bar{X}$ charts, for $ATS_0 = 370.4$, $ASI_0 = 1$, $n = 5$, and $\delta \in \{-2.00, -1.50, -1.00, -0.75, -0.50, -0.25, -0.10, 0.10, 0.25, 0.50, 0.75, 1.00, 1.50, 2.00\}$, when $(h_S, h_L) \in \{(0.1, 1.5), (0.1, 1.9), (0.1, 4.0)\}$ and $\lambda = 0.5$ under Gamma (4, 1), Gamma (2, 1), and Gamma (1, 1) distributions

	Shewhart $\bar{X}$	EWMA $\bar{X}$	VSI EWMA $\bar{X}$		
(h_S, h_L)	(1.0, 1.0)	(1.0, 1.0)	(0.1, 1.5)	(0.1, 1.9)	(0.1, 4.0)
δ	Gamma (4, 1)				
	Upper One-sided Charts				
	$K^+ = 3.2848$	$K^+ = 3.2482$	$(W^+, K^+) = (0.6364, 3.2206)$	$(W^+, K^+) = (0.6011, 3.1282)$	$(W^+, K^+) = (0.6264, 2.7766)$
	(ATS_1, $SDTS_1$)	(ATS_1, $SDTS_1$)	(ATS_1, $SDTS_1$)	(ATS_1, $SDTS_1$)	(ATS_1, $SDTS_1$)
0.10	(230.65, 230.15)	(181.31, 179.62)	(155.55, 155.93)	(156.39, 156.95)	(167.33, 168.68)
0.25	(116.44, 115.94)	(65.16, 63.23)	(39.75, 40.03)	(40.23, 40.69)	(48.44, 49.69)
0.50	(40.31, 39.81)	(15.80, 13.75)	(4.30, 4.42)	(4.38, 4.66)	(6.41, 7.48)
0.75	(15.57, 15.06)	(6.11, 4.24)	(0.88, 0.97)	(0.88, 1.09)	(1.30, 2.16)
1.00	(6.81, 6.29)	(3.39, 1.80)	(0.31, 0.40)	(0.30, 0.45)	(0.37, 0.93)
1.50	(2.01, 1.42)	(1.80, 0.66)	(0.08, 0.07)	(0.07, 0.07)	(0.05, 0.09)
2.00	(1.12, 0.37)	(1.25, 0.43)	(0.02, 0.04)	(0.02, 0.04)	(0.01, 0.03)
	Lower One-sided Charts				
	$K^- = 2.2861$	$K^- = 2.4648$	$(W^-, K^-) = (0.6172, 2.4660)$	$(W^-, K^-) = (0.6455, 2.4057)$	$(W^-, K^-) = (0.6472, 2.2151)$
	(ATS_1, $SDTS_1$)	(ATS_1, $SDTS_1$)	(ATS_1, $SDTS_1$)	(ATS_1, $SDTS_1$)	(ATS_1, $SDTS_1$)
–0.10	(132.29, 131.78)	(100.37, 98.12)	(82.58, 82.87)	(87.68, 88.09)	(103.92, 105.05)
–0.25	(38.30, 37.79)	(24.29, 22.19)	(14.10, 14.40)	(16.03, 16.47)	(23.08, 24.30)
–0.50	(8.87, 8.36)	(6.30, 4.60)	(2.05, 2.37)	(2.45, 2.93)	(4.14, 5.39)
–0.75	(3.49, 2.95)	(3.17, 1.81)	(0.61, 0.92)	(0.73, 1.17)	(1.25, 2.34)
–1.00	(1.96, 1.37)	(2.11, 1.02)	(0.24, 0.48)	(0.28, 0.62)	(0.46, 1.28)
–1.50	(1.17, 0.44)	(1.31, 0.51)	(0.05, 0.16)	(0.05, 0.21)	(0.07, 0.43)
–2.00	(1.02, 0.16)	(1.06, 0.25)	(0.01, 0.05)	(0.01, 0.07)	(0.01, 0.13)

continue to next page

continue from previous page

	Gamma (2, 1)				
	Upper One-sided Charts				
	$K^+ = 3.4912$	$K^+ = 3.4150$	$(W^+, K^+) = (0.6268, 3.3833)$	$(W^+, K^+) = (0.6089, 3.2730)$	$(W^+, K^+) = (0.6121, 2.8915)$
	$(ATS_1, SDTS_1)$	$(ATS_1, SDTS_1)$	$(ATS_1, SDTS_1)$	$(ATS_1, SDTS_1)$	$(ATS_1, SDTS_1)$
0.10	(243.26, 242.76)	(195.63, 194.04)	(168.22, 168.63)	(169.54, 170.11)	(178.10, 179.50)
0.25	(131.72, 131.22)	(76.12, 74.25)	(46.29, 46.59)	(47.21, 47.67)	(54.25, 55.52)
0.50	(49.86, 49.36)	(19.13, 17.05)	(4.83, 4.89)	(4.98, 5.19)	(6.71, 7.73)
0.75	(20.31, 19.80)	(7.14, 5.19)	(0.93, 0.94)	(0.94, 1.07)	(1.23, 2.01)
1.00	(9.02, 8.50)	(3.79, 2.10)	(0.33, 0.37)	(0.32, 0.41)	(0.33, 0.80)
1.50	(2.47, 1.90)	(1.92, 0.69)	(0.09, 0.07)	(0.08, 0.07)	(0.06, 0.06)
2.00	(1.19, 0.47)	(1.33, 0.47)	(0.03, 0.05)	(0.03, 0.04)	(0.01, 0.03)
	Lower One-sided Charts				
	$K^- = 2.0876$	$K^- = 2.3177$	$(W^-, K^-) = (0.6510, 2.3169)$	$(W^-, K^-) = (0.6434, 2.2691)$	$(W^-, K^-) = (0.6620, 2.0991)$
	$(ATS_1, SDTS_1)$	$(ATS_1, SDTS_1)$	$(ATS_1, SDTS_1)$	$(ATS_1, SDTS_1)$	$(ATS_1, SDTS_1)$
–0.10	(103.92, 103.42)	(84.49, 82.14)	(69.50, 69.76)	(73.93, 74.32)	(91.38, 92.43)
–0.25	(26.14, 25.63)	(19.37, 17.29)	(11.39, 11.69)	(12.88, 13.33)	(19.70, 20.90)
–0.50	(6.14, 5.62)	(5.35, 3.75)	(1.84, 2.19)	(2.15, 2.65)	(3.81, 5.08)
–0.75	(2.68, 2.12)	(2.83, 1.58)	(0.59, 0.92)	(0.68, 1.14)	(1.23, 2.33)
–1.00	(1.67, 1.06)	(1.93, 0.94)	(0.24, 0.51)	(0.27, 0.64)	(0.47, 1.33)
–1.50	(1.12, 0.37)	(1.25, 0.47)	(0.04, 0.19)	(0.05, 0.23)	(0.07, 0.48)
–2.00	(1.02, 0.14)	(1.05, 0.22)	(0.01, 0.07)	(0.01, 0.08)	(0.01, 0.17)

continue to next page

continue from previous page

	Gamma (1, 1)				
	Upper One-sided Charts				
	$K^+ = 3.7792$	$K^+ = 3.6491$	$(W^+, K^+) = (0.6439, 3.5989)$	$(W^+, K^+) = (0.6218, 3.4721)$	$(W^+, K^+) = (0.6119, 3.0413)$
	$(ATS_1, SDTS_1)$	$(ATS_1, SDTS_1)$	$(ATS_1, SDTS_1)$	$(ATS_1, SDTS_1)$	$(ATS_1, SDTS_1)$
0.10	(258.03, 257.53)	(213.67, 212.21)	(185.87, 186.31)	(186.61, 187.21)	(192.85, 194.30)
0.25	(151.42, 150.92)	(91.98, 90.22)	(57.18, 57.48)	(57.69, 58.14)	(63.46, 64.72)
0.50	(64.04, 63.53)	(24.71, 22.62)	(5.84, 5.82)	(5.86, 5.97)	(7.25, 8.15)
0.75	(28.21, 27.70)	(8.95, 6.90)	(1.06, 0.98)	(1.03, 1.05)	(1.18, 1.83)
1.00	(13.06, 12.55)	(4.48, 2.65)	(0.37, 0.35)	(0.34, 0.37)	(0.30, 0.61)
1.50	(3.43, 2.88)	(2.10, 0.74)	(0.11, 0.07)	(0.10, 0.07)	(0.07, 0.06)
2.00	(1.36, 0.70)	(1.45, 0.50)	(0.04, 0.05)	(0.04, 0.05)	(0.02, 0.04)
	Lower One-sided Charts				
	$K^- = 1.8200$	$K^- = 2.1222$	$(W^-, K^-) = (0.6500, 2.1240)$	$(W^-, K^-) = (0.6911, 2.0812)$	$(W^-, K^-) = (0.6388, 1.9518)$
	$(ATS_1, SDTS_1)$	$(ATS_1, SDTS_1)$	$(ATS_1, SDTS_1)$	$(ATS_1, SDTS_1)$	$(ATS_1, SDTS_1)$
–0.10	(64.57, 64.07)	(64.18, 61.75)	(52.00, 52.24)	(57.37, 57.71)	(73.61, 74.71)
–0.25	(14.21, 13.70)	(14.18, 12.15)	(8.26, 8.57)	(9.83, 10.27)	(15.25, 16.49)
–0.50	(3.82, 3.29)	(4.34, 2.87)	(1.52, 1.91)	(1.88, 2.41)	(3.21, 4.50)
–0.75	(1.99, 1.41)	(2.44, 1.34)	(0.52, 0.88)	(0.65, 1.13)	(1.11, 2.22)
–1.00	(1.42, 0.77)	(1.72, 0.84)	(0.22, 0.51)	(0.27, 0.66)	(0.45, 1.32)
–1.50	(1.08, 0.30)	(1.18, 0.42)	(0.04, 0.21)	(0.05, 0.27)	(0.08, 0.53)
–2.00	(1.02, 0.13)	(1.04, 0.20)	(0.01, 0.08)	(0.01, 0.11)	(0.01, 0.22)

–1.00, the lower one-sided VSI EWMA $\bar{X}$ charts with λ = 0.2 and $(h_S, h_L) \in$ { (0.1, 1.5), (0.1, 1.9), (0.1, 4.0)} have (ATS_1, $SDTS_1$) ∈ {(0.37, 0.57), (0.41, 0.69), (0.67, 1.49)}, respectively, which are lower than (ATS_1, $SDTS_1$) = (1.96, 1.37), and (2.77, 0.91) of the lower one-sided Shewhart $\bar{X}$ and EWMA $\bar{X}$ charts, respectively (Table 4). However, there are exceptions in some cases when δ –0.10 under the lower one-sided VSI EWMA $\bar{X}$ chart with (h_S, h_L) = (0.1, 4.0). This may be due to the use of a large sampling interval h_L in the warning region of the chart, leading to a longer time to detect a signal for small negative mean shifts. In terms of the λ value, it is found that when λ = 0.1, the lower one-sided VSI EWMA $\bar{X}$ chart with (h_S, h_L) = (0.1, 1.5) exhibits the fastest detection speed compared to the lower one-sided Shewhart $\bar{X}$, EWMA $\bar{X}$ and other combinations of VSI EWMA $\bar{X}$ charts in detecting small levels of negative mean shifts (δ -0.25) across all the gamma distributions (Tables 3 - 5). For $\delta \geq$ = - 0.50, the lower one-sided VSI EWMA $\bar{X}$ chart with λ = 0.2 and (h_S, h_L) = (0.1, 1.5) generally outperforms other competing charts for all the gamma distributions (Table 4). When monitoring moderate to large shift sizes (-2.00 ≤ δ ≤- 0.75), the combination of λ = 0.5 and (h_S, h_L) = (0.1, 1.5) for the lower one-sided VSI EWMA $\bar{X}$ chart proves to be the most efficient chart, surpassing the lower one-sided Shewhart $\bar{X}$, EWMA $\bar{X}$ and other combinations of VSI EWMA $\bar{X}$ charts across all the gamma distributions (Table 5).

AN ILLUSTRATIVE APPLICATION

This section illustrates a practical example for the application of the upper one-sided VSI EWMA $\bar{X}$ chart under the gamma distribution for monitoring the weight of bias tyres in a scooter manufacturing process. This real-life example is adopted from Lee et al. (2022). A bias tyre, also known as a bias-ply tyre, for a scooter is a type of tyre construction where the layers of fabric or plies are laid diagonally from bead to bead at angles typically between 30 and 40 degrees to the centreline of the tyre. The weight of the bias tyre is a significant quality characteristic that needs to be monitored to ensure that the production of scooters meets manufacturers' quality standards, to prevent delays or issues on the assembly line, and to reduce defects or returns. Therefore, it is essential to monitor the weight of bias tyres to achieve quality assurance and operational efficiency. Lee et al. (2022) determined that the weight data for bias tires are modelled by a gamma distribution with a shape parameter a = 2 and a scale parameter b = 1. These parameters were subsequently used for further calculations in this example.

In our example, the process parameters a and b are directly sourced from the work of Lee et al. (2022), so no further estimation of the parameters is necessary. However, to provide a complete procedure for estimating and choosing the parameters a and b form real data, some additional methods are elaborated in this paragraph. When selecting the parameters a and b form real data, a practitioner would typically rely on empirical evidence from the process being monitored. In practical scenarios, one might analyse historical process data (often referred to as Phase-I data) to estimate the distribution parameters and validate whether the underlying assumption about the data distribution holds true. Statistical methods such as maximum likelihood estimation or moment estimation are commonly employed to determine these parameters based on available statically stable and in-control historical data (Wu et al. 2020). Once the parameters have been estimated, some specifications must be set for computing the proposed chart's control limits, such as the ATS_0, ASI_0, n, λ and δ for the VSI EWMA $\bar{X}$ chart. Practitioners can use different ATS_0 and ASI_0 values to find an appropriate balance between false alarm rates and detection speed, ensuring the chart is customised to the specific need of their process. A smaller sample size n is typically chosen in industry settings where collecting larger samples may not be feasible. For the selection of λ, practitioners can select based on the desired sensitivity to small or large shifts, while δ can be chosen according to the actual situation of the real process.

To proceed with this illustrative example, by using a = 2 and b = 1 as obtained from Lee et al. (2022), the process parameters are calculated as $\mu_0 = 2 \times 1 = 2.0000$ kg and $\sigma_0 = \sqrt{2 \times 1^2} = 1.4142$ kg. Table 6 shows the complete summary statistics for the simulated weight of bias tyres from a scooter manufacturing process. The samples for the first 11 subgroups (from i = 1 to 11) are simulated under the in-control case, whereas the subsequent samples (from i = 12 to 25) are simulated under the out-of-control condition with δ = 0.50. In Table 6, the out-of-control points are indicated by the boldfaced values. For illustration, we assume that ATS_0 = 370.4, ASI_0 = 1, n = 5, λ = 0.1, and δ = 0.50 for the upper one-sided VSI EWMA $\bar{X}$ chart with (h_S, h_L) = (0.1, 1.5). Since the data follow a Gamma (2, 1) distribution, we can directly obtain the corresponding new charting parameters from Table 3, which are (W^+, K^+) = (0.6167, 2.8552). Using Equations (2) and (3) with these charting parameters, the upper warning and control limits are then calculated as UWL = $2 + 0.6167 \times \sqrt{0.1/(5 \times (2 - 0.1))} \times 1.4142 = 2.0895$ and UCL = $2 + 2.8552 \times \sqrt{0.1/(5 \times (2 - 0.1))} \times 1.4142 = 2.4143$, respectively. Note that the centre limit is calculated as CL = μ_0 = 2.0000. Figure 5 displays the plot of the upper one-sided VSI EWMA $\bar{X}$ chart with (h_S, h_L) = (0.1, 1.5), for monitoring the weight of bias tyres in the scooter manufacturing process.

Referring to Table 6, the plotting statistics Z_i^+ of the upper one-sided VSI EWMA $\bar{X}$ chart with (h_S, h_L) = (0.1, 1.5) are determined using Equation (1). The working mechanism of the upper one-sided VSI EWMA $\bar{X}$ chart

with (h_S, h_L) = (0.1, 1.5) is described as follows. From Figure 5, the first sample (i = 1), with i = 2.0061 locates in the safe region [CL, UWL]. Consequently, the next sample (i = 2) is obtained after h_L = 1.5 time units, which corresponds to the long sampling interval. This procedure resumes until the 12th sample, where its Z_{12}^{+} = 2.1199 positions in the warning region (UWL, UCL]. As a result, the subsequent sample (i = 13) is obtained after h_S = 0.1 time units, corresponding to the short sampling interval. The determination of the next sampling interval proceeds until Z_{20}^{+} exceeds the UCL = 2.4143, signalling the first out-of-control status at the 20th sample, with a total elapsed time of 17.30 time units. Quality engineers immediately investigate the assignable cause and address it swiftly to restore the process to its in-control operating conditions. The remaining out-of-control conditions occur at samples 21 - 25 (Table 6 & Figure 5).

Additionally, from Figure 5, h_L is used during the in-control case because the process is stable. However, starting

TABLE 6. Summary statistics for the weight of bias tyres (in kilograms, kg) from a scooter manufacturing process

Sample Number, i	$\bar{X}_i$	Z_i^+	Sampling interval, h_S or h_L (time unit)	Total Elapsed Time (time unit)
1	2.0605	2.0061	1.5	0.00
2	1.2902	2.0000	1.5	1.50
3	2.2573	2.0257	1.5	3.00
4	2.2048	2.0436	1.5	4.50
5	1.3415	2.0000	1.5	6.00
6	2.6191	2.0619	1.5	7.50
7	1.6586	2.0216	1.5	9.00
8	2.1135	2.0308	1.5	10.50
9	1.1382	2.0000	1.5	12.00
10	1.7668	2.0000	1.5	13.50
11	0.7198	2.0000	1.5	15.00
12	3.1994	2.1199	0.1	16.50
13	2.4571	2.1537	0.1	16.60
14	3.4354	2.2818	0.1	16.70
15	2.5976	2.3134	0.1	16.80
16	2.6079	2.3429	0.1	16.90
17	1.4618	2.2548	0.1	17.00
18	2.7219	2.3015	0.1	17.10
19	2.6067	2.3320	0.1	17.20
20	4.0709	**2.5059**	*	17.30
21	3.6003	**2.6153**		
22	2.3997	**2.5938**		
23	2.2395	**2.5583**		
24	2.8629	**2.5888**		
25	2.7468	**2.6046**		

Remarks: The boldfaced values refer to the out-of-control points

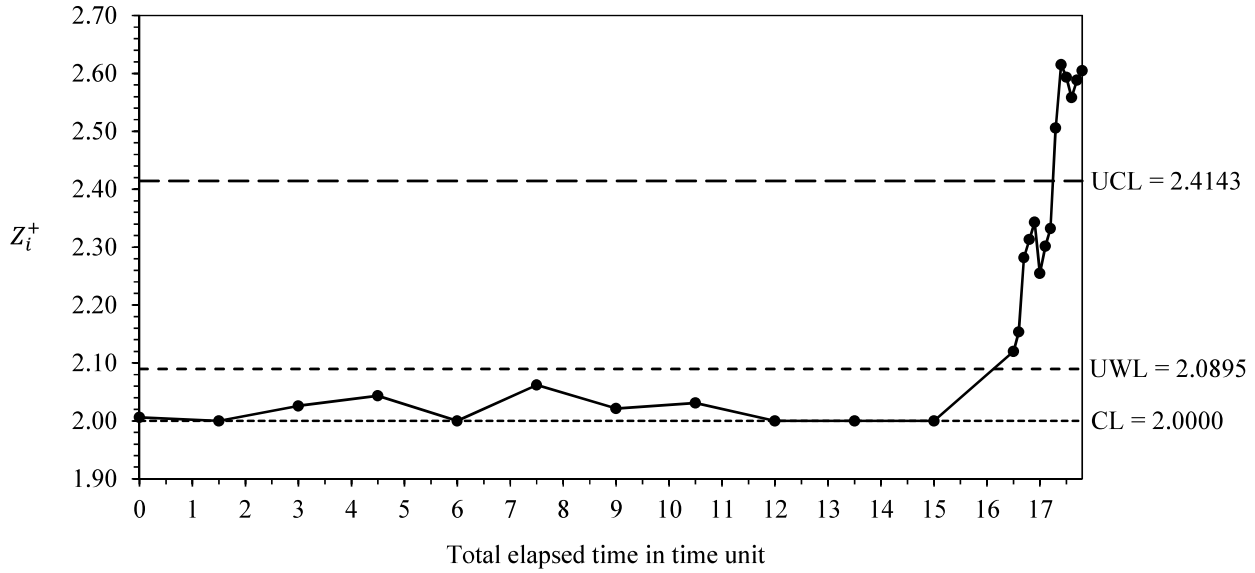

FIGURE 5. The upper one-sided VSI EWMA $\bar{X}$ chart with (h_S, h_L) = (0.1, 1.5), for monitoring the weight of bias tyres (in kilograms, kg) from a scooter manufacturing process

from the 12th sample (corresponding to a total elapsed time of 16.50 time units) onwards, h_S is employed as the plot shows an increasing trend, signalling the potential occurrence of out-of-control conditions. In fact, the out-of-control condition begins from 12th sample onwards, which is simulated using δ = 0.5. From this example of application, it is evident that the VSI EWMA $\bar{X}$ chart adopts h_L to reduce sampling costs when the process is stable and switches to h_S to enhance its detection efficiency when the process becomes unstable and out-of-control.

CONCLUSIONS

This paper conducts a thorough assessment to investigate the effectiveness of the one-sided VSI EWMA $\bar{X}$ charts that were developed based on the normal distribution model, particularly when the process distribution is characterised by a gamma distribution. Analysis of in-control performances clearly indicates that as the degree of skewness for the gamma distribution increases, the upper one-sided VSI EWMA $\bar{X}$ chart issues excessive false alarms. Conversely, the lower one-sided VSI EWMA $\bar{X}$ charts require a longer time (much larger than 370.4) to produce signals as skewness increases, potentially increasing the sampling cost for practitioners in process monitoring. These two issues are problematic for practitioners because they lead to inefficiencies in the quality control process during practical applications.

To deal with these problems, we propose new charting parameters for both the upper and lower one-sided VSI EWMA $\bar{X}$ charts, which are specifically designed under the gamma distribution. We also provide and tabulate a range of potential values for these charting parameters as a reference and guide for practitioners in future construction of the proposed VSI EWMA $\bar{X}$ control chart. Moreover, with respect to detecting small levels of positive (or negative) mean shifts, the upper (or lower) one-sided VSI EWMA $\bar{X}$ chart with (h_S, h_L) = (0.1, 1.5) and λ = 0.1 demonstrates the best detection performance compared to the upper (or lower) one-sided Shewhart $\bar{X}$, EWMA $\bar{X}$ and other combinations of VSI EWMA $\bar{X}$ charts across all the specified gamma distributions. For moderate levels of positive (or negative) process mean shifts, the upper (or lower) one-sided VSI EWMA $\bar{X}$ chart with (h_S, h_L) = (0.1, 1.5) and λ = 0.2 generally outperforms other comparing charts for all the gamma distributions. When monitoring large levels of positive (or negative) mean shifts, the upper (or lower) one-sided VSI EWMA $\bar{X}$ chart with (h_S, h_L) = (0.1, 1.5) and λ = 0.5 remains the most efficient chart compared to the Shewhart $\bar{X}$, EWMA $\bar{X}$, and other combinations of VSI EWMA $\bar{X}$ charts across all the gamma distributions. Therefore, this paper strongly shows that the proposed one-sided VSI EWMA $\bar{X}$ control charts demonstrate high effectiveness and efficiency in the gamma process monitoring. A practical illustration is provided to showcase the applicability and practicality of the proposed one-sided VSI EWMA $\bar{X}$ chart under the gamma distribution. This includes some valuable insights on selecting appropriate parameters *a* and *b* for real industry data and determining the specifications necessary for effective implementation. By offering clear guidelines for charting parameters selection, it will not only enhance the reliability of the control chart, but also enable practitioners to customise the chart to meet their specific needs, ultimately resulting in more efficient process monitoring and improved quality outcomes.

Future investigations could develop theoretical frameworks and optimisation algorithms tailored specifically for the one-sided VSI EWMA $\bar{X}$ charts that conform to the gamma distribution, to achieve more effective process monitoring and enhanced efficiency. As an alternative, this research could be expanded to examine other non-normal or skewed distributions, including the log-normal and Weibull distributions. These efforts would enable the development of advanced control charts that are adaptable to a broader range of manufacturing and quality assurance environments.

ACKNOWLEDGEMENTS

This research was funded and supported by the Ministry of Higher Education (MOHE), Malaysia through the Fundamental Research Grant Scheme (FRGS) No. FRGS/1/2021/STG06/HWUM/02/1.

REFERENCES

Bai, Y., Chiang, J.Y., Liu, W. & Mou, Z. 2024. An enhanced EWMA chart with variable sampling interval scheme for monitoring the exponential process with estimated parameters. *Scientific Reports* 14(4): 7958.

Brook, D. & Evans, D.A. 1972. An approach to the probability distribution of CUSUM run length. *Biometrika* 59(3): 539-549.

Borror, C.M., Montgomery, D.C. & Runger, G.C. 1999. Robustness of the EWMA control chart to non-normality. *Journal of Quality Technology* 31(3): 309-316.

Chakraborti, S. & Graham, M.A. 2019. Nonparametric (distribution-free) control charts: An updated overview and some results. *Quality Engineering* 31(4): 523-544.

Chakraborti, S., Van Der Laan, P. & Bakir, S.T. 2001. Nonparametric control charts: An overview and some results. *Journal of Quality Technology* 33(3): 304-315.

Chou, Y.M., Polansky, A.M. & Mason, R.L. 1998. Transforming non-normal data to normality in statistical process control. *Journal of Quality Technology* 30(2): 133-141.

Deenen, P.C., Middelhuis, J., Akcay, A. & Adan, I.J.B.F. 2024. Data-driven aggregate modelling of a semiconductor wafer fab to predict WIP levels and cycle time distributions. *Flexible Services and Manufacturing* 36(6): 567-596.

Hamasha, M.M., Ali, H., Hamasha, S. & Ahmed, A. 2022. Ultra-fine transformation of data for normality. *Heliyon* 8(5): e09370.

Haq, A. & Akhtar, S. 2022. Auxiliary information based maximum EWMA and DEWMA charts with variable sampling intervals for process mean and variance. *Communications in Statistics – Theory and Methods* 51(12): 3985-4005.

Hu, X., Zhang, S., Xie, F. & Song, Z. 2024. Triple exponentially weighted moving average control charts without or without variable sampling interval for monitoring the coefficient of variation. *Journal of Statistical Computation and Simulation* 94(3): 536-570.

Hu, X., Zhang, J., Zhang, S., Zhou, P. & Zhang, Y. 2023. A variable sampling interval one-sided CUSUM control chart for monitoring the multivariate coefficient of variation. *Journal of King Saud University – Science* 35(7): 102845.

Kao, S. & Ho, C. 2006. Process monitoring of the sample variances through an optimal normalizing transformation. *The International Journal of Advanced Manufacturing Technology* 30(5): 459-469.

Khoo, M.B.C., Saha, S., Lee, H.C. & Castagliola, P. 2019. Variable sampling interval exponentially weighted moving average median chart with estimated process parameters. *Quality and Reliability Engineering International* 35(8): 2732-2748.

Li, C.I., Su, N.C., Su, P.F. & Shyr, Y. 2014. The design of $\bar{X}$ and R control charts for skew normal distributed data. *Communications in Statistics – Theory and Methods* 43(23): 4908-4924.

Lee, P. & Zhang, H. 2020. The design of $\bar{X}$ chart when the mean and parameters of gamma distribution change. *2020 International Conference on Modern Education and Information Management (ICMEIM)* 2020(1): 538-542.

Lee, P.H., Torng, C.C., Lin, C.H. & Chou, C.Y. 2022. Control chart pattern recognition using spectral clustering technique and support vector machine under gamma distribution. *Computers & Industrial Engineering* 171(9): 108437.

Liu, Y., Liu, Y. & Jung, U. 2020. Nonparametric multivariate control chart based on density-sensitive novelty weight for non-normal processes. *Quality Technology & Quantitative Management* 17(2): 203-215.

Madrid-Alvarez, H.M., García-Díaz, J.C. & Tercero-Gómez, V.G. 2024. A CUSUM control chart for gamma distribution with guaranteed performance. *Quality and Reliability Engineering International* 40(3): 1279-1301.

Nawaz, M.S., Azam, M. & Aslam, M. 2021. EWMA and DEWMA repetitive control charts under non-normal processes. *Journal of Applied Statistics* 48(1): 4-40.

Noorossana, R., Fathizadan, S. & Nayebpour, M.R. 2016. EWMA control chart performance with estimated process parameters under non-normality. *Quality and Reliability Engineering International* 32(5): 1637-1654.

Parvin, R., Khoo, M.B.C., Saha, S. & Teoh, W.L. 2023. Proposed variable sampling interval maximum EWMA and distance EWMA charts with unknown process parameters. *Stat* 12(1): e605.

Reynolds, M.R., Amin, R.W., Arnold, J.C. & Nachlas, J.A. 1988. $\bar{X}$ charts with variable sampling intervals. *Technometrics* 30(2): 181-192.

Sabahno, H. & Eriksson, M. 2024. Variable parameters memory-type control charts for simultaneous monitoring of the mean and variability of multivariate multiple linear regression profiles. *Scientific Reports* 12(4): 9288.

Sanmugan, K. & Muzalwana, A.T. 2022. Insights into variations in COVID-19 infections in Malaysia. *Sains Malaysiana* 51(5): 1599-1608.

Teh, S.Y., Khoo, M.B.C., Ong, K.S., Soh, K.L. & Teoh, W.L. 2015. A study on the -EWMA chart for monitoring the process variance based on the MRL performance. *Sains Malaysiana* 44(7): 1067-1075.

Teoh, J.W., Teoh, W.L., Chong, Z.L., Lee, M.H. & Khaw, K.W. 2024. A robust design for the omnibus SPRT control chart under skewed data distributions. *Sains Malaysiana* 53(6): 1441-1461.

Teoh, W.L., Ong, L.V., Khoo, M.B.C., Castagliola, P. & Chong, Z.L. 2021. The variable sampling interval EWMA $\bar{X}$ chart with estimated process parameters. *Journal of Testing and Evaluation* 49(2): 1237-1265.

Teoh, W.L., Yeong, W.C., Khoo, M.B.C. & Teh, S.Y. 2016. The performance of the double sampling $\bar{X}$ chart with estimated process parameters for skewed distributions. *Academic Journal of Science* 5(1): 237-252.

Tran, K.D., Nguyen, H.D., Nguyen, T.H. & Tran, K.P. 2020. Design of a variable sampling interval exponentially weighted moving average median control chart in presence of measurement errors. *Quality and Reliability Engineering International* 37(1): 374-390.

Wang, Y., Hu, X., Zhou, X., Qiao, Y. & Wu, S. 2020. New one-sided EWMA *t* charts without and with variable sampling intervals for monitoring the process mean. *Mathematical Problems in Engineering* 2020(1): 7567215.

Wu, Y., Younas, S., Abbas, K., Ali, A. & Khan, S.A. 2020. Monitoring reliability for three-parameter Frechet distribution using control charts. *IEEE Access* 8(1): 71245-71253.

Xie, F., Castagliola, P., Li, Z., Sun, J. & Hu, X. 2022. One-sided adaptive truncated exponentially weighted moving average $\bar{X}$ schemes for detecting process mean shifts. *Quality Technology & Quantitative Management* 19(5): 533-561.

Yeong, W.C., Khoo, M.B.C., Tham, L.K., Teoh, W.L. & Rahim, M.A. 2017. Monitoring the coefficient of variation using a variable sampling interval EWMA chart. *Journal of Quality Technology* 49(4): 380-401.

*Corresponding author; email: wei_lin.teoh@hw.ac.uk